On the Singlet-Exciton States of Crystalline Anthracene

ROBERT SILBEY,* JOSHUA JORTNER, AND STUART A. RICE
Department of Chemistry and Institute for the Study of Metals, University of Chicago, Chicago, Illinois
(Received 6 July 1964)

In this paper we present a detailed analysis of the lower excited states of crystalline anthracene. Starting with zero-order product wavefunctions, the treatment differs from standard formulations in that interactions between molecules are computed directly by the use of π-electron theory, by the inclusion of the effects of extensive configuration mixing, and by the inclusion of long-range interactions out to the convergence limit. It is found that:

(1) The computation of interaction energies cannot be reduced to dipole–dipole terms alone. By the use of π-electron theory it is shown that short-range high-order multipole (greater than dipole) interactions make important contributions to both the diagonal and off-diagonal elements of the energy matrix.

(2) Long-range interactions of the dipole–dipole type are of importance for distances of the order of the wavelength of light. By application of momentum-conservation conditions, it is shown that the long-range dipole–dipole interactions, including the effects of retardation of the potential, are absolutely convergent. Major contributions to the Davydov splitting arise from molecular separations ranging from 50 Å to the convergence limit.

(3) For the case of allowed singlet–singlet transitions, electron-exchange interactions are small relative to other contributions to the interaction energy.

(4) Under the experimental conditions used to date, the Davydov splitting should be independent of crystal thickness.

(5) In anthracene, crystal-field mixing of the p and β molecular states has a large effect on the Davydov splitting. Inclusion of mixing with higher excited π states has little effect on the Davydov splitting, but is required in the calculation of the polarization ratios in the vibronic components of the p band.

(6) Charge-transfer exciton states play only a minor role in altering the properties of singlet exciton states arising from allowed transitions.

(7) The detailed calculations reported herein yield good agreement with the observed Davydov splitting (ΔE) and polarization (P) ratios in anthracene, e.g., for the $^1A_{1g}\rightarrow{}^1B_{2u}$ band:

Vibronic band	ΔE(calc.) (cm^{-1})	ΔE(obs.) (cm^{-1})	P(calc.)	P(obs.)
0–0	207	230	3.5	5
0–1	102	145	2.5	4.5
0–2	54	80	1.9	3

I. INTRODUCTION

THE theory of light absorption by molecular crystals was first studied by Frenkel[1] and Peierls[2] and has since been extended by many workers.[3] The conventional theory is based on the observation that molecular crystals are held together by weak dispersion forces so that, to a first approximation, the manifold of electronic states of each molecule can be considered to be unaltered by the crystal field. Because of the small but finite intermolecular forces, it is impossible to construct a stationary state for a perfect crystal in which some one selected molecule is excited. The correct zero-order states for the crystal with one quantum of electronic excitation correspond to a delocalization of the electronic energy over all molecules. It is convenient to describe the quantum of excitation as an exciton wave of momentum $\hbar\mathbf{k}$ which propagates through the crystal with a velocity determined by the intermolecular interaction.

Now, aromatic compounds have a number of electronic transitions for which the spatial extent of the electron density is almost the same in both the ground state and the excited state. In this case, with overlap integrals between molecular orbitals on adjacent molecules of the order of 10^{-2} to 10^{-3}, considerable simplification of the analysis is feasible. For, in the case of small intermolecular overlap, the Heitler–London formalism may be used to construct proper zero-order wavefunctions. Following the pioneering work of Davydov,[3a] the Heitler–London scheme has often been used to construct both the ground-state and excited-state wavefunctions, and much effort has gone into calculations of energy shifts and splittings associated with the interaction of a molecule and the weak crystal field.[3] Advantage is also taken of the small intermolecular overlap to represent the interaction between molecules in a multipole expansion. Usually only dipole terms in the expansion are retained, although some recent work has dealt with octopole contributions.[3b,4]

* National Science Foundation Cooperative Fellow.

[1] J. Frenkel, Phys. Rev. **37**, 17 (1931).

[2] R. Peierls, Ann. Physik **13**, 905 (1932).

[3] (a) A. S. Davydov, *Theory of Molecular Excitons* (McGraw-Hill Book Company, Inc., New York 1962); (b) D. Fox and O. Schnepp, J. Chem. Phys. **23**, 767 (1955); (c) D. S. McClure, Solid State Phys. **8**, 1 (1959); (d) D. P. Craig and S. H. Walmsley, *Physics and Chemistry of the Organic Solid State*, edited by M. M. Labes, D. Fox, and A. Weissberger (John Wiley & Sons, Inc., New York, 1963), Vol. 1, p. 585.

[4] T. A. Claxton, D. P. Craig, and T. Thirunamachandran, J. Chem. Phys. **35**, 1525 (1961).

The work presented in this paper draws heavily on previous research. There are, however, two notable differences between our analysis and the previous work. First, π-electron theory has progressed to such an extent that we feel it may be profitably applied to the present problem, thereby bypassing use of the multipole expansion. In the work reported here the intermolecular interactions are computed using the best available π-electron wavefunctions, and direct calculations are carried out to relatively large distances ($\sim$50 Å). These calculations make possible the evaluation of short-range interactions. Second, in the region from 50 Å to the bounding surfaces, dipole sums are used. In previous work, Craig and Walsh[5] made use of the Ewald–Kornfeld procedure for evaluating dipole sums (characterized by $\mathbf{k}=\mathbf{0}$ and neglecting retardation of the interaction), comparing this result with a finite summation which counted all the dipole–dipole interactions within a sphere of radius 20–30 Å. This procedure is open to serious criticism: It is well known that dipole sums are only conditionally convergent,[6] since an interaction of the form $(\cos\vartheta_{ij}-3\cos\vartheta_i\cos\vartheta_j)R_{ij}^{-3}$ decreases with increasing R_{ij} only as fast as the volume of space (number of interacting molecules) increases. The dipole sums for $\mathbf{k}=\mathbf{0}$, in general, depend on the shape of the solid. In examining only the case $\mathbf{k}=\mathbf{0}$, the momentum of the photon ($\hbar\mathbf{q}$) is neglected. In addition, retardation of the interaction between molecules is neglected. This approximation is equivalent to the assumption that all the transition dipoles in the crystal are in phase and that they interact instantaneously. Momentum conservation requires (when the interaction between the radiation field and the phonon field is neglected) that $\mathbf{k}=\mathbf{q}$. The ratio of $\mathbf{k}$ to the magnitude of the primitive translation vector of the reciprocal lattice of the crystal is of the order of 10^{-3}, and the assumption $\mathbf{k}=\mathbf{0}$ is justified only for short-range interactions, i.e., octopole–octopole or electron-exchange interactions. The dependence of the dipole sums on the direction of the propagation vector of the exciton has been discussed by Fox and Yatsiv.[7] We shall demonstrate that introduction of the momentum conservation restriction and the effects of retardation of the interaction imply that the dipole sums become absolutely convergent for an infinite crystal and independent of boundary conditions.

II. FORMULATION OF THE THEORY

The theory of molecular excitons has been treated in many articles.[3] Nevertheless it is advantageous to sketch briefly the principles involved as used in the work reported here.

The Hamiltonian for a crystal containing N unit cells and h molecules per unit cell may be written in the form

$$\mathcal{H}=\sum_{\mu=1}^{h}\sum_{k=1}^{N}H_{k\mu}+\sum_{k\mu<l\nu}V_{k\mu,l\nu}, \tag{1}$$

where the double indices $k\mu$ and $l\nu$ label different molecules, $H_{k\mu}$ is the Hamiltonian for an isolated molecule, and $V_{k\mu,l\nu}$ is the intermolecular pair interaction. Since the coupling between molecules is small compared with intramolecular interactions, the Heitler–London formalism may be used in this problem. The ground state of the crystal is, then, represented in the form

$$\Psi^0=\mathcal{A}\prod\varphi_{k\mu}{}^0, \tag{2}$$

where the $\varphi_{k\mu}{}^0$ are the ground-state (antisymmetrized) wavefunctions of the individual molecules and $\mathcal{A}$ is the antisymmetrization operator permuting electrons between the molecules.

The wavefunctions corresponding to the fth excited state of the crystal are, in the same formalism,

$$\Psi_i{}^f=h^{-\frac{1}{2}}\sum_{\alpha=1}^{h}B_\alpha{}^i\Phi_\alpha{}^f, \tag{3}$$

$$\Phi_\alpha{}^f=\left(\frac{h}{N}\right)^{\frac{1}{2}}\sum_{m=1}^{N}\exp(i\mathbf{k}\cdot\mathbf{r}_{m\alpha})\phi_{m\alpha}{}^f, \tag{4}$$

$$\phi_{m\alpha}{}^f=\mathcal{A}\varphi_{m\alpha}{}^f\prod_{l\nu\neq m\alpha}{}'\varphi_{l\nu}{}^0. \tag{5}$$

The functions $\Phi_\alpha{}^f$ are known as one-site excitons, $\mathbf{r}_{m\alpha}$ is the vector from the origin to the center of the molecule $m\alpha$, and the coefficients $B_\alpha{}^i$ can be found by diagonalizing the $h\times h$ secular determinant or by using the symmetry properties of the group of the wave vector.

For the case where there exists one state for each representation of the factor group the energies of the Davydov components of this excited state, relative to the ground state, are given by

$$E_f{}^i=E_f{}^0+D_f+M_f{}^i(\mathbf{k}); \qquad i=1,\cdots,h. \tag{6}$$

In Eq. (6), $E_f{}^0$ is the excitation energy of the free molecule and D_f represents the energy shift of the center of gravity of the band:

$$D_f=\sum_m\sum_\mu(\langle\mathcal{A}\varphi_{n\nu}{}^f\varphi_{n\nu}{}^f\mid V_{n\nu,m\mu}\mid\varphi_{m\mu}{}^0\varphi_{m\mu}{}^0\rangle - \langle\mathcal{A}\varphi_{n\nu}{}^0\varphi_{n\nu}{}^0\mid V_{n\nu,m\mu}\mid\varphi_{m\mu}{}^0\varphi_{m\mu}{}^0\rangle). \tag{7}$$

Since D_f leads to a uniform shift of all the energy levels, it may be thought of as an environmental effect. On the other hand, $M_f{}^i(\mathbf{k})$ is different for each representation of the factor group and thereby leads to the splitting of the crystal level into h components (Davydov splitting):

$$M_f{}^i=\sum_{m\neq n}\sum_\mu\{(B_\nu{}^i)^*B_\mu{}^i\exp[i(\mathbf{k}\cdot(\mathbf{r}_{n\nu}-\mathbf{r}_{m\mu})]\times\langle\mathcal{A}\varphi_{n\nu}{}^f\varphi_{m\mu}{}^0\mid V_{n\nu,m\mu}\mid\varphi_n{}^{\nu0}\varphi_{m\mu}{}^f\rangle\}. \tag{8}$$

In Eq. (8), $n\nu$ is an arbitrarily chosen reference molecule. The coefficients $B_\nu{}^i$ and $B_\mu{}^i$ are obtained by diagonal-

[5] D. P. Craig and J. R. Walsh, J. Chem. Soc. **1958**, 1613.
[6] M. H. Cohen and F. Keffer, Phys. Rev. **99**, 1128 (1955).
[7] D. Fox and S. Yatsiv, Phys. Rev. **108**, 938 (1957).

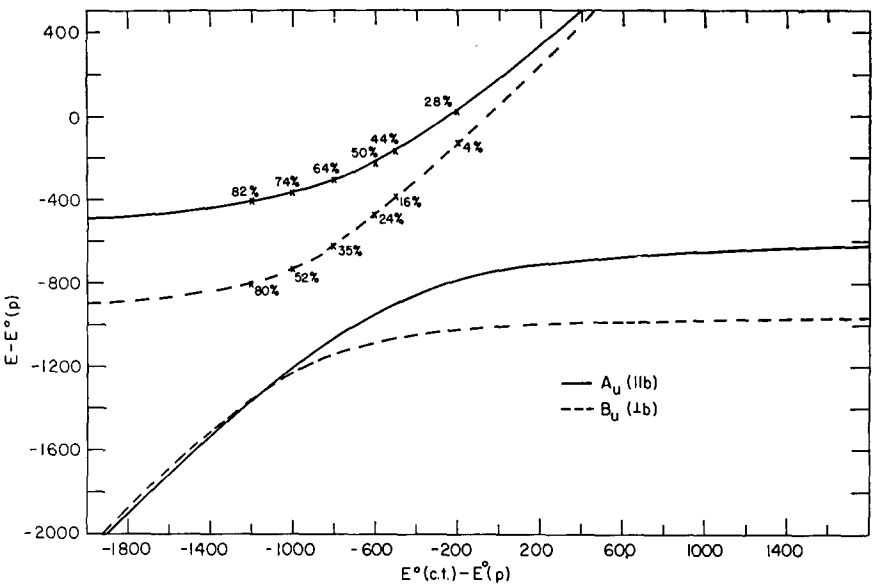

FIG. 1. Energies of states with respect to p state vs energy of charge-transfer state with respect to p state. Numbers are percentage of p character in state.

izing the tight-binding Hamiltonian (1) with the basis set (3).

The compound to which we apply our analysis (anthracene) crystallizes in the monoclinic system with space group C_{2h}^5 and has two molecules per unit cell. Corresponding to every excited state, it is possible to form a one-site exciton for each site in the unit cell. We denote these one-site excitons by $\Phi_1^f(\mathbf{k})$ and $\Phi_2^f(\mathbf{k})$. An elementary argument leads to the linear combinations

$$\Psi_-^f(\mathbf{k})=(1/\sqrt{2})[\Phi_1^f(\mathbf{k})-\Phi_2^f(\mathbf{k})]$$

and

$$\Psi_+^f(\mathbf{k})=(1/\sqrt{2})[\Phi_1^f(\mathbf{k})+\Phi_2^f(\mathbf{k})]. \quad (9)$$

The vectors defining the unit cell are **a, b,** and **c** (see Fig. 1). In this crystal lattice a Type 1 molecule may be transformed into a Type 2 molecule by reflection in the ac place followed by a glide of $\frac{1}{2}\mathbf{a}$. At $\mathbf{k}=\mathbf{0}$ the group of the wave vector is isomorphous with the group C_{2h} whose character table is displayed in Table I. For the case of dipole radiation, the allowed symmetry types are A_u (polarized parallel to **b**) and B_u (polarized perpendicular to **b**). Now,

$$\sigma_{ac}{}^{fg}\Phi_1^f=\Phi_2^f \quad (10)$$

and

$$i\Phi_1^f=-\Phi_1^f,$$

$$i\Phi_2^f=-\Phi_2^f. \quad (11)$$

Equations (11) follow from the observation that all the excited states of interest to us are odd with respect to inversion since the molecular point group is D_{2h}, and the identity and inversion operations of D_{2h} and C_{2h} are identical. By comparison of Eqs. (9)–(11) and Table I, it is seen that $\Psi_-^f(\mathbf{0})$ is of type A_u and $\Psi_+^f(\mathbf{0})$ is of type B_u. The reader should note that this assignment agrees with that of Craig,[3d,6] but not that of Davydov.[3a] Davydov makes the (unjustified) assumption that $C_2{}^{fg}$ has a relationship to C_2 in the molecular point group (D_{2h}). When $\mathbf{k}\neq\mathbf{0}$, the symmetries of $\Psi_-^f(\mathbf{k})$ and $\Psi_+^f(\mathbf{k})$ depend on the group of the wave vector. For example, when **k** is parallel to **b** this group is C_2, and $\Psi_-^f(\mathbf{k})$ for u states is of the B type while $\Psi_+^f(\mathbf{k})$ is of Type A.

We have considered thus far only the formal outline of the analysis. Using a more detailed representation of the molecular wavefunctions, and when only one excited state is considered, the excited-state wavefunctions are

$$\Psi_\pm^f(\mathbf{k})=\sum_n \exp(i\mathbf{k}\cdot\mathbf{r}_{n1})$$

$$\times(\mathcal{A}\varphi_{n1}^f\prod_{mj\neq n1}\varphi_{mj}{}^0\pm\exp(i\mathbf{k}\cdot\boldsymbol{\tau})\mathcal{A}\varphi_{n2}^f\prod_{mj\neq n2}\varphi_{mj}{}^0), \quad (12)$$

where $\boldsymbol{\tau}=\frac{1}{2}(\mathbf{a}+\mathbf{b})$. The exciton band structure is determined by

$$M_f^\pm=E_\pm^f(\mathbf{k})$$

$$=\sum_{m1;m\neq n}(J_{n1,m1}{}^f+K_{n1,m1}{}^f)\exp[i\mathbf{k}\cdot(\mathbf{r}_{m1}-\mathbf{r}_{n1})]$$

$$\pm\sum_{m2}(J_{n1,m2}{}^f+K_{n1,m2}{}^f)\exp[i\mathbf{k}\cdot(\mathbf{r}_{m2}-\mathbf{r}_{n1})], \quad (13)$$

where the excitation-transfer matrix element is

$$J_{n1,m\mu}{}^f=\langle\varphi_{n1}{}^f\varphi_{m\mu}{}^0\mid V_{n1,m\mu}\mid\varphi_{n1}{}^0\varphi_{m\mu}{}^f\rangle, \quad (14)$$

while the electron and excitation-exchange matrix

TABLE I. Character table for the group C_{2h}.

	E	$C_2{}^{fg}$	i	$\sigma_{ac}{}^{fg}$
A_g	1	1	1	1
A_u	1	1	−1	−1
B_g	1	−1	1	−1
B_u	1	−1	−1	1

element is

$$K_{n1,m\mu}{}^{f}=\langle[\sum_{P}(-1)^{P}P-1]\varphi_{n1}{}^{f}\varphi_{m\mu}{}^{0}\mid V_{n1,m\mu}\mid\varphi_{n1}{}^{0}\varphi_{m\mu}{}^{f}\rangle. \tag{15}$$

Only terms involving excitation transfer and electron exchange between translationally nonequivalent molecules lead to a Davydov splitting, while interactions between translationally equivalent molecules contribute to the band shift. The Davydov splitting, in first order, is given by

$$\Delta E^{f}=E_{+}{}^{f}(\mathbf{k})-E_{-}{}^{f}(\mathbf{k}), \tag{16}$$

and, bearing in mind the necessity for momentum conservation ($\mathbf{k}=\mathbf{q}$), we obtain

$$\Delta E^{f}=2\sum_{m2}(J_{n1,m2}{}^{f}+K_{n1,m2}{}^{f})\exp[i\mathbf{q}\cdot(\mathbf{r}_{m2}-\mathbf{r}_{n1})]. \tag{17}$$

The exciton theory just sketched must be extended by taking into account crystal-field-induced mixing of excited molecular states into the state f. The tight-binding Hamiltonian (1) must be diagonalized in the basis set $\Psi^{f}(\mathbf{k})$, where the indices f refer to all the molecular excited states. The diagonal matrix elements are obtained from Eqs. (6) and (13). The off-diagonal elements assume the form:

$$\mathcal{H}_{fg}{}^{\pm}=\langle\Psi_{\pm}{}^{f}(\mathbf{k})\mid\mathcal{H}\mid\Psi_{\pm}{}^{g}(\mathbf{k})\rangle, \tag{18}$$

$$\mathcal{H}_{fg}{}^{\pm}=\sum_{m1\neq n1}\Gamma_{m1,n1}{}^{fg}\cos[(\mathbf{r}_{n1}-\mathbf{r}_{m1})\cdot\mathbf{k}]$$

$$\pm\sum_{m2}\Gamma_{m2,n1}{}^{fg}\cos[(\mathbf{r}_{n1}-\mathbf{r}_{m2})\cdot\mathbf{k}]+\sum_{mi\neq n1}\Delta_{mi,n1}{}^{fg}, \tag{19}$$

where

$$\Gamma_{m1,ni}{}^{fg}=\tfrac{1}{2}(\langle\mathcal{A}\varphi_{n1}{}^{f}\varphi_{mi}{}^{0}\mid V_{n1,mi}\mid\varphi_{n1}{}^{0}\varphi_{mi}{}^{g}\rangle$$

$$+\langle\mathcal{A}\varphi_{n1}{}^{0}\varphi_{mi}{}^{f}\mid V_{n1,mi}\mid\varphi_{n1}{}^{g}\varphi_{mi}{}^{0}\rangle), \tag{20}$$

$$\Delta_{mi,n1}{}^{fg}=\tfrac{1}{2}(\langle\mathcal{A}\varphi_{n1}{}^{f}\varphi_{mi}{}^{0}\mid V_{n1,mi}\mid\varphi_{n1}{}^{g}\varphi_{mi}{}^{0}\rangle$$

$$+\langle\mathcal{A}\varphi_{n1}{}^{0}\varphi_{mi}{}^{f}\mid V_{ni,mi}\mid\varphi_{n1}{}^{0}\varphi_{mi}{}^{g}\rangle). \tag{21}$$

III. EVALUATION OF THE MATRIX ELEMENTS

To reduce Eqs. (13)–(21) to numerical form, both the intermolecular potential and the molecular wavefunctions must be specified. The intermolecular pair potential has the form

$$V_{k,l}=\sum_{I,J}\frac{Z_{I}Z_{J}e^{2}}{R_{IJ}}-\sum_{I,j}\frac{Z_{I}e^{2}}{R_{Ij}}-\sum_{J,i}\frac{Z_{J}e^{2}}{R_{Ji}}+\sum_{i>j}\frac{e^{2}}{r_{ij}}, \tag{22}$$

where I and J refer to nuclei in the different molecules k and l, i refers to the electrons on k, and j to the electrons on l.

In previous applications of exciton theory to the singlet excited states of aromatic crystals, the following procedure has usually been adopted:

(a) A multiple expansion for the matrix elements of V_{kl} is introduced and the series truncated after only a few (usually the dipole) terms.

(b) The polarization of the transition is chosen on the basis of experimental or theoretical arguments.

(c) The dipole terms are evaluated using the experimental oscillator strength (obtained from solution spectra).

(d) For allowed optical transitions, the higher multipoles are not calculated. Some calculations have been reported[5,8] in which the octopole transition moment is used as a variable parameter to obtain agreement with experiment. It is not apparent without detailed calculation how many terms have to be included in the multipole expansion. Similar problems are encountered in the computation of dispersion forces between aromatic molecules.[9]

(e) The dipole sum is often truncated at a relatively small distance. The inadequacy of this calculation has already been mentioned.[7]

In the present work we attempt to evaluate the matrix elements of V_{kl} to distances of the order of 50 Å using the best available π-electron wavefunctions. For larger distances, the dipole summation will be used. We now turn to the choice of molecular wavefunctions. The molecular wavefunctions used were antisymmetrized products of Hückel molecular orbitals and semiempirical configuration-interaction wavefunctions in the π-electron approximation computed by Pariser.[10] The relevant molecular states and the wavefunctions used are entered in Table II.

The J and K integrals required for the calculation of the first-order Davydov splitting can now be represented in terms of the molecular wavefunctions. Using Hückel wavefunctions, these integrals for the $^{1}B_{2u}(p)$ excited state assume the form:

$$J_{n1,m\mu}{}^{p}=2\langle u_{m\mu}{}^{7}(1)u_{m\mu}{}^{8}(1)\mid r_{12}{}^{-1}\mid u_{n1}{}^{7}(2)u_{n1}{}^{8}(2)\rangle,$$

$$\equiv 2\langle u_{m\mu}{}^{7}u_{m\mu}{}^{8}\mid u_{n1}{}^{7}u_{n1}{}^{8}\rangle, \tag{23}$$

$$K_{m\mu}{}^{p}=-\langle u_{m\mu}{}^{7}(1)u_{n1}{}^{7}(1)\mid r_{12}{}^{-1}\mid u_{m\mu}{}^{8}(2)u_{n1}{}^{8}(2)\rangle$$

$$\equiv-\langle u_{m\mu}{}^{7}u_{n1}{}^{7}\mid u_{m\mu}{}^{8}u_{n1}{}^{8}\rangle, \tag{24}$$

where $u_{a}{}^{i}$ represents the molecular orbital i located on Molecule a.

Somewhat more complex expressions are obtained using the configuration-interaction (Pariser) wavefunctions. For the $^{1}B_{2u}(p)$ and $^{1}B_{3u}(\beta)$ states, the

[8] D. P. Craig and S. H. Walmsley, Mol. Phys. **4**, 113 (1961).
[9] P. L. Davies and C. A. Coulson, Trans. Faraday Soc. **48**, 777 (1952).
[10] R. Pariser, J. Chem. Phys. **24**, 250 (1956).

TABLE II. Molecular wavefunctions for anthracene.

State	Wavefunction[a]	f_{calc}[b]	f_{exptl}[c]	Energy (exptl.)[c] (cm^{-1})	Source
	W_0			0	Hückel
$^1A_{1g}$	$0.99618W_0-(0.00801/2)(W_{7-11}-W_{4-8})$ $-(0.07416/2)(W_{6-10}-W_{5-9})-(0.0895/2)(W_{7-14}-W_{1-8})$ $+(0.03473/2)(W_{3-11}-W_{4-12})-(0.02780/2)(W_{2-10}$ $-W_{5-13})$				Pariser[d]
	W_{7-8}	0.51	0.10	26 500	Hückel
$^1B_{2u}(p)$	$0.98214W_{7-8}+0.14921W_{6-9}-0.03911W_{5-10}$ $(-0.10772/\sqrt{2})(W_{7-12}+W_{3-8})$	0.386	0.10		Pariser[b]
	$\frac{1}{2}(W_{6-8}+W_{7-9})$	3.5	2.3	39 000	Hückel
$^1B_{3u}(\beta)$	$(0.97085/2)(W_{6-8}+W_{7-9})+(0.21720/2)(W_{5-11}+W_{4-10})$ $-(0.03045/2)(W_{3-9}W_{6-12})-(0.09668/2)(W_{7-11}+W_{2-8})$	3.23	2.3		Pariser[b]

[a] The wavefunctions W represent antisymmetrized singlet states being eigenfunctions of $S^2=0$. W_0 is the ground-state wavefunction, while W_{ij} represents an excited configuration due to one-electron excitation from Orbital i to Orbital j. The molecular orbitals are labeled 1 to 14 in the order of inreasing energy.
[b] Calculated oscillator strengths from Ref. d.
[c] Experimental transition energies and oscillator strengths taken from H. B. Klevens and J. R. Platt, J. Chem. Phys. **17**, 470 (1949).
[d] R. Pariser, J. Chem. Phys. **24**, 324 (1956). We are grateful to Pariser for providing us with the unpublished anthracene functions.

excitation-transfer matrix elements can be represented in the form

$$J_{n1,m\mu}{}^{p}=1.9292\langle u_{m\mu}{}^{7}u_{m\mu}{}^{8}\mid u_{n1}{}^{7}u_{n1}{}^{8}\rangle+0.29310(\langle u_{m\mu}{}^{7}u_{m\mu}{}^{8}\mid u_{n1}{}^{6}u_{n1}{}^{9}\rangle+\langle u_{m\mu}{}^{6}u_{m\mu}{}^{9}\mid u_{n1}{}^{7}u_{n1}{}^{8}\rangle)$$
$$-0.29920(\langle u_{m\mu}{}^{7}u_{m\mu}{}^{8}\mid u_{n1}{}^{3}u_{n1}{}^{8}\rangle+\langle u_{m\mu}{}^{8}u_{m\mu}{}^{3}\mid u_{n1}{}^{7}u_{n1}{}^{8}\rangle)-0.07682(\langle u_{m\mu}{}^{7}u_{m\mu}{}^{8}\mid u_{n1}{}^{5}u_{n1}{}^{10}\rangle+\langle u_{m\mu}{}^{5}u_{m\mu}{}^{10}\mid u_{n1}{}^{7}u_{n1}{}^{8}\rangle)$$
$$+0.08892\langle u_{m\mu}{}^{6}u_{m\mu}{}^{9}\mid u_{n1}{}^{6}u_{n1}{}^{9}\rangle+0.04640\langle u_{m\mu}{}^{8}u_{m\mu}{}^{3}\mid u_{n1}{}^{8}u_{n1}{}^{3}\rangle \quad (25)$$

and

$$J_{n1,m\mu}{}^{\beta}=3.7702\langle u_{m\mu}{}^{8}u_{m\mu}{}^{6}\mid u_{n1}{}^{6}u_{n1}{}^{8}\rangle+0.84348(\langle u_{m\mu}{}^{8}u_{m\mu}{}^{6}\mid u_{n1}{}^{4}u_{n1}{}^{10}\rangle+\langle u_{m\mu}{}^{4}u_{m\mu}{}^{10}\mid u_{n1}{}^{8}u_{n1}{}^{6}\rangle)$$
$$-0.37544(\langle u_{m\mu}{}^{6}u_{m\mu}{}^{8}\mid u_{n1}{}^{2}u_{n1}{}^{8}\rangle+\langle u_{m\mu}{}^{2}u_{m\mu}{}^{8}\mid u_{n1}{}^{6}u_{n1}{}^{8}\rangle)+0.18872\langle u_{m\mu}{}^{4}u_{m\mu}{}^{10}\mid u_{n1}{}^{4}u_{n1}{}^{10}\rangle$$
$$-0.11824(\langle u_{m\mu}{}^{6}u_{m\mu}{}^{8}\mid u_{n1}{}^{3}u_{n1}{}^{9}\rangle+\langle u_{m\mu}{}^{3}u_{m\mu}{}^{9}\mid u_{n1}{}^{6}u_{n1}{}^{8}\rangle)-0.08400(\langle u_{m\mu}{}^{4}u_{m\mu}{}^{10}\mid u_{n1}{}^{2}u_{n1}{}^{8}\rangle+\langle u_{m\mu}{}^{2}u_{m\mu}{}^{8}\mid u_{n1}{}^{4}u_{n1}{}^{10}\rangle). \quad (26)$$

The molecular orbitals u^m are now represented in terms of a linear combination of carbon-atom $2pz$ wavefunctions ω^i:

$$u^m=\sum_i \omega^i C_i{}^n, \quad (27)$$

where the $C_i{}^n$ are Hückel coefficients without overlap. Using these functions, the matrix elements are reduced to Coulomb integrals:

$$\langle u_{m\mu}{}^{7}u_{m\mu}{}^{8}\mid u_{n1}{}^{7}u_{n1}{}^{8}\rangle=\sum_{i,j,k,l} C_i{}^{7}C_j{}^{8}C_k{}^{7}C_l{}^{8}\langle \omega_{m\mu}{}^{i}(1)\omega_{m\mu}{}^{8}(1)\mid 1/r_{12}\mid \omega_{n1}{}^{k}(2)\omega_{n1l}(2)\rangle. \quad (28)$$

In the calculations reported herein, three- and four-center integrals are neglected. Order-of-magnitude estimates based on the Mulliken approximation indicate that the contribution of these high-order terms will not exceed 10%. The calculation of the Coulomb integrals requires proper choice of the carbon-atom wavefunctions. Unlike the case of electron-exchange[11] and charge-transfer[12] interactions, these Coulomb integrals are not sensitive to the behavior of the molecular wavefunctions at large distances. However, in order to obtain maximum accuracy, SCF $2p$ carbon-atom wavefunctions were used for the computation of the Coulomb integrals. The same wavefunctions were used for the computation of the exchange integrals $K_{n1,m\mu}{}^{f}$ previously described.[11]

The matrix elements necessary for the computation of the energy shifts and splittings were computed directly using an IBM 7094. The details of these computations are described in Appendix I. The interactions calculated for the inner zone were extended to

[11] J. L. Katz, J. Jortner, S. I. Choi, and S. A. Rice, J. Chem. Phys. **39**, 1897 (1963).
[12] S. I. Choi, J. Jortner, S. A. Rice, and R. Silbey, J. Chem. Phys. **41**, 3294 (1964).

TABLE III. Single first-order exciton-interaction terms for anthracene crystal (all energies in cm^{-1}).

	Translationally inequivalent molecules					Translationally equivalent molecules				
(a) Anthracene—p band										
1. Spherical convergence										
R	$I_{dd}{}^{p}$	HU	δHU	PA	δPA	$I_{d-d}{}^{p}$	HU	δHU	PA	δPA
20	35	−267	−442	−99	−235	−334	−1114	556	−1025	280
25	36	−266	−446	−97	−237	−369	−1278	567	−1140	299
30	26	−313	−443	−131	−242	−362	−1248	570	−1116	295
35	30	−294	−444	−118	−235	−377	−1317	568	−1167	303
40	57	−162	−447	−24	−246	−399	−1424	570	−1242	314
45	81	−46	−451	+55	−259	−427	−1561	574	−1339	326
50	90	44	−451	120	−266	−449	−1603	582	−1410	341
55	100	89	−456	153	−273	−457	−1694	591	−1433	349
60	110	95	−455	157	−272	−457	−1704	583	−1439	343
65	110	91	−459	154	−275	−457	−1702	583	−1439	343
2. Slab convergence										
No. of cells										
2	−169	−1257	−405	−796	−137	−287	−889	546	−861	258
3	−134	−1080	−410	−674	−152	−300	−948	552	−905	265
4	−71	−777	−422	−460	−190	−351	−1195	560	−1080	289
5	−19	−527	−432	−282	−204	−336	−1120	560	−1027	283
6	+27	−302	−437	−124	−229	−428	−1566	574	−1342	325
7	+72	−85	−445	+30	−250	−426	−1556	574	−1340	321
8	+110	88	−462	+152	−277	−457	−1702	583	−1438	343
(b) Anthracene—β band										
1. Spherical convergence										
R	$I_{dd}{}^{\beta}$	HU		PA		$I_{d-d}{}^{\beta}$	HU		PA	
20	7833	7 990		8 293		3853	2655		2767	
25	7245	7 278		7 677		4542	3490		3665	
30	7140	7 131		7 518		4473	3430		3607	
35	7542	7 641		8 067		4470	3402		3581	
40	8178	8 452		8 940		5083	4200		4030	
45	8867	9 234		9 880		5708	4995		5286	
50	9405	10 007		10 613		6100	5501		5871	
55	9736	10 430		11 070		6323	5785		6135	
60	9911	10 650		11 307		6429	5918		6353	
65	9980	10 736		11 400		6482	5986		6280	
2. Slab convergence										
No. of cells										
2	4765	4 104		4 259		3000	1636		1675	
3	5682	5 281		5 526		3762	2548		2653	
4	7134	7 122		7 508		5024	4140		4366	
5	8279	8 578		9 075		5459	4693		4963	
6	9111	9 633		10 210		6233	5672		6016	
7	9625	10 290		10 918		6254	5700		6045	
8	9980	10 801		11 460		6487	6003		6370	

about 60 Å in all directions thereby including approximately 2000 molecules. The interactions summed over translationally equivalent and translationally nonequivalent molecules are displayed in Table III. Here HU and PA represent the interactions calculated using the Hückel and Pariser wavefunctions. It is important to note at this point that both wavefunctions overestimate the transition dipole moment to the $^1B_{2u}(p)$ state, and therefore a scaling procedure must be devised to correct the calculated matrix elements. In Table III we compare the total interaction matrix-element sums with the first term of the monopole expansion, i.e., the static dipole–dipole sums over the same region:

$$I_{dd}=\sum_{m\mu}\exp[\mathbf{q}\cdot(\mathbf{r}_{m\mu}-\mathbf{r}_{n1})]\times\left\{\frac{\mathbf{\mu}_{n1}\cdot\mathbf{\mu}_{m\mu}}{|\mathbf{r}_{m\mu}-\mathbf{r}_{n1}|^3}-\frac{3[\mathbf{\mu}_{n1}\cdot(\mathbf{r}_{m\mu}-\mathbf{r}_{n1})][\mathbf{\mu}_{m\mu}\cdot(\mathbf{r}_{m\mu}-\mathbf{r}_{n1})]}{|r_{m\mu}-r_{n1}|^5}\right\}. \tag{29}$$

In Eq. (31), $\mathbf{\mu}$ represents the transition dipole moment. For short-range interactions $\mathbf{q}\cdot(\mathbf{r}_{m\mu}\cdot\mathbf{r}_{n1})\approx 0$, and the modulation and retardation of the dipole–dipole sums are irrelevant.

Recent work on rutile[13] has shown that dipole sums within a sphere tend to oscillate about a limit, while sums within a slab the shape of the unit cell tend to a limit more regularly. For this reason, we have carried out the dipole sums needed to estimate the multipole interaction in both geometries.

The contribution I_m of higher-order multipoles (greater than dipoles) to the interaction energy may be computed by subtracting from the inner zone total interaction energy, the interaction energy due to just the transition dipoles. The latter must be scaled by a numerical factor C which is the ratio between the squares of the calculated and experimental transition moments of the free molecule. For the p state of anthracene, from Table II, we take $C_{\mathrm{HW}}=5$ for the Hückel and $C_{\mathrm{A}}=3.9$ for the Pariser wavefunction. Thus, the contribution of the higher multipoles is given by $\delta_{\mathrm{HU}}=\mathrm{HU}-5I_{dd}$ and $\delta_{\mathrm{PA}}=\mathrm{PA}-3.9I_{dd}$ for Hückel and Pariser wavefunctions, respectively. It is found that the higher-multipole interaction contribution in the anthracene p band is of short range, as expected. To obtain the correct energy, it is necessary to scale the magnitude of the higher multipoles. As seen from Table III the higher-multipole contributions computed on the Hückel basis and the Pariser basis show that the entire multipole expansion for the $^1B_{2u}(p)$ state scales just as do the dipole–dipole sums, so that the contributions of the higher multipoles in the p band is just $I_m=\mathrm{PA}/3.9-I_{dd}$, and $I_m=-92\ \mathrm{cm}^{-1}$.

In the $^1B_{3u}(\beta)$ intense band, the computed interaction energies were sensibly independent of the wavefunctions used for the computations. Since the dipole moment corresponding to this transition is very large, the dipole–dipole terms are dominant while the contribution of higher multipoles is less than 10%. The $^1B_{3u}$ results were therefore left as computed.

IV. EVALUATION OF LONG-RANGE INTERACTIONS

We now consider the interactions at intermolecular pair separations greater than 50 Å. As shown in the last section, these long-range interactions are due only to dipole–dipole terms. It has been demonstrated (by Heller and Marcus[14]) that the contribution of dipole–dipole interactions between distant neighbors cannot be neglected for small values of $\mathbf{q}$.

In our treatment of long-range interactions a continuum model introduced by Heller and Marcus was extended to the case of more than 1 molecule per unit. We shall consider again the + and − states of the crystal as linear combinations of unit-cell wavefunctions $(1/\sqrt{2})[\phi_{m1}\pm\exp(i\mathbf{k}\cdot\boldsymbol{\tau})\phi_{m2}]\exp(i\mathbf{k}\cdot\mathbf{r}_{m1})$. An application of the multipole expansion to the interaction matrix element on the basis of the unit-cell functions leads to the interaction of unit-cell transition dipoles, $\cdots$. It is seen that the − state dipole is oriented along the $\mathbf{b}$ axis, and the + state dipole is oriented in the plane perpendicular to the $\mathbf{b}$ axis. We shall consider only the dipole–dipole interaction in this scheme. Since the minimum distance between molecules is of the order of 50 Å, it is assumed that the contribution of higher multipoles has converged within the inner excluded region.

Because the wavefunctions belong to different irreducible representations, the + and − states do not interact with light whose $\mathbf{k}$ vector is parallel to $(\mathbf{b})^{-1}$ or perpendicular to $(\mathbf{b})^{-1}$. Therefore we need consider only the case of interaction between parallel dipoles,

$$I_{dd}=\sum_{i;R>R_0}\exp(i\mathbf{k}\cdot\mathbf{R}_i)\left\{\frac{\mu_i^2R_i^2-3(\boldsymbol{\mu}_i\cdot\mathbf{R}_i)^2}{R_i^5}(\cos kR_i+kR_i\sin kR_i)+k^2\left[\frac{(\boldsymbol{\mu}_i\cdot\mathbf{R}_i)^2-\mu_i^2R_i^2}{R_i^3}\right]\cos kR_i\right\},\qquad(30)$$

with $\boldsymbol{\mu}$ the dipole moment of the unit cell. Now the unit cell is small relative to the volume excluded from (30) ($\sim$125 Å^3 compared with $\sim125\times10^3$ Å^3), so that the sum may be replaced by an integral over a density of dipoles. Of course, the direct summation for the inner volume must be added to complete the evaluation of the total interaction energy. Indeed, as shown, within this volume we have included all interactions. For the region outside R_0, Eq. (30) becomes

$$I_{dd}=(8\pi/3V)\,|\,\boldsymbol{\mu}\,|^2P_2(\cos\boldsymbol{\mu}\cdot\mathbf{k})+(4\pi/3V)\,|\,\boldsymbol{\mu}^2\,|\,[P_2(\cos\boldsymbol{\mu}\cdot\mathbf{k})+1]\sin^2kR_f,\qquad(31)$$

where V is the volume of a unit cell, P_2 is the second Legendre polynomial, and the second term on the right-hand side of (31) is a boundary term arising from retardation effects. It is shown in Appendix II, that this boundary term is small compared to the static dipole term ($\sim$20% or less) and may be neglected to the accuracy of the calculations reported herein. The reader can find in Appendix II, a derivation of Eq. (30), which is written for the case that the inner zone is a sphere, along with a discussion of retardation effects.

Consider the two transition moments

$$\boldsymbol{\mu}_{A_u}=\frac{1}{\sqrt{2}}(\mathbf{p}_1-\mathbf{p}_2)=\sqrt{2}\begin{pmatrix}0\\ b\\ 0\end{pmatrix}|\,\mathbf{p}\,|$$

and

$$\boldsymbol{\mu}_{B_u}=\frac{1}{\sqrt{2}}(\mathbf{p}_1+\mathbf{p}_2)=\sqrt{2}\begin{pmatrix}a\\ 0\\ c\end{pmatrix}|\,\mathbf{p}\,|,\qquad(32)$$

[13] H. C. Bolton, W. Fawcett, and D. C. Gurney, Proc. Phys. Soc. (London) **A80**, 199 (1962).

[14] W. Heller and A. Marcus, Phys. Rev. **84**, 809 (1951).

TABLE IV. Long-range dipole–dipole contribution to the Davydov splitting and band shift in anthracene[a] (energies in cm^{-1}).

Transition	Polarization axis	$\sum_{m1} J_{n1,m1}$ (equiv.)	$\sum_{m2} J_{n1,m2}$ (inequiv.)
$^1A_{1g} \rightarrow {}^1B_{2u}(p)$	short	−250	+316
$^1A_{1g} \rightarrow {}^1B_{3u}(\beta)$	long	6435	6600

[a] These data were computed using the experimental values for the oscillator strengths.

where (a, b, c) is the vector representing the direction cosines of the transition dipole of Molecule 1 in the unit cell, and $|\mathbf{p}|$ is the magnitude of the transition dipole. Then, in view of the discussion in Appendix II,

$$S_{A_u}{}^p = |\mathfrak{y}_{A_u}|^2(8\pi/3V)\,P_2(\cos\mathfrak{y}_{A_u}\cdot\mathbf{k})[j_0(kR_0)+j_2(kR_0)]$$

and

$$S_{B_u}{}^p = |\mathfrak{y}_{B_u}|^2(8\pi/3V)\,P_2(\cos\mathfrak{y}_{B_u}\cdot\mathbf{k})[j_0(kR_0)+j_2(kR_0)]. \quad (33)$$

From the definitions, it readily follows that the contributions of the long-range dipole–dipole sums over translationally equivalent and nonequivalent molecules are given by

$$\sum_{m1\neq n1} J_{n1,m1}{}^p \cos(\mathbf{k}\cdot\mathbf{r}_{m1}) = \tfrac{1}{2}(S_{A_u}{}^p + S_{B_u}{}^p)$$

and

$$\sum_{m2} J_{n1,m2}\cos(\mathbf{k}\cdot\mathbf{r}_{m2}) = \tfrac{1}{2}(S_{B_u}{}^p - S_{A_u}{}^p) \quad (34)$$

for $R > R_0$. Here the superscript p refers to the contribution to the diagonal matrix element for the $^1B_{2u}(p)$ state. Since the excluded volume is characterized by a radius $R_0 \approx 50$ Å, $kR_0 \approx 0.2$ and $j_0(kR_0)+j_2(kR_0) \approx 1$. We shall limit ourselves to the case wherein the $\mathbf{k}$ vector is perpendicular to the ab plane, so that $\mathbf{k} \,||\, (\mathbf{c}')^{-1}$. This is the case of practical interest, as all experimental results have been obtained for $\mathbf{k}$ along the normal to the $(ab)^{-1}$ plane. It is found that

$$\cos(\mathfrak{y}_{A_u}\cdot\mathbf{k}) = 0; \qquad P_2[\cos(\mathfrak{y}_{A_u}\cdot\mathbf{k})] = -\tfrac{1}{2}$$

and

$$\cos(\mathfrak{y}_{B_u}\cdot\mathbf{k}) = c/(a^2+c^2)^{\frac{1}{2}};$$

$$P_2[\cos(\mathfrak{y}_{B_u}\cdot\mathbf{k})] = (2c^2-a^2)/2(a^2+c^2), \quad (35)$$

whereupon

$$S_{B_u}+S_{A_u} = \tfrac{8}{3}\pi(|\mathbf{p}|^2/V)(3c^2-1)$$

and

$$S_{B_u}-S_{A_u} = \tfrac{8}{3}\pi(|\mathbf{p}|^2/V)(2c^2+b^2-a^2). \quad (36)$$

Using the crystal data cited in Appendix IV, the long-range contributions to the Davydov splitting can be obtained. These results are displayed in Table IV.

It should be noted that a substantial contribution to the factor-group splitting arises from the external region.

V. CRYSTAL-FIELD MIXING

The first-order theory described in Sec. II is not sufficient to account for the Davydov splittings and intensity ratios in aromatic crystals. The importance of configuration interaction between singlet exciton states arising from crystal-field perturbations was first pointed out by Craig.[15] Moreover, as pointed out by Fox and Yatsiv,[7] the off-diagonal matrix elements of the Hamiltonian are extremely important when long-range interactions are included.

In the analysis reported here, we have considered the configuration interaction between the anthracene p and β states, which requires the evaluation of the integrals $\Gamma_{m1,n1}{}^{p\beta}$, $\Gamma_{m2,n1}{}^{p\beta}$, and $\Delta_{n1,mi}{}^{p\beta}$ [Eqs. (18) and (19)]. Previous work has employed the multipole expansion for the pair-interaction term, keeping only the dipole–dipole interaction. In this approximation the $\Delta_{n1,mi}(i=1, 2)$ matrix elements vanish.[15] Using the MO π-electron scheme, we write, in the Hückel approximation,

$$\Delta_{nm} = \sum_{r=1}^{7}(\langle u_n{}^8 u_n{}^9 \,|\, u_m{}^r u_m{}^r\rangle - \langle u_n{}^6 u_n{}^7 \,|\, u_m{}^r u_m{}^r\rangle). \quad (37)$$

Neglecting the contribution of three- and four-center integrals and assuming the validity of the pairing property for the molecular orbitals of an alternant hydrocarbon, we get $\Delta_{nm}=0$.

The $\Gamma_{nm}{}^{p\beta}$ integrals were evaluated numerically for molecules within a sphere of 50 Å. The matrix elements take the form

$$\Gamma_{nm}{}^{p\beta} = (1/\sqrt{2})(\langle u_n{}^8 u_n{}^6 \,|\, u_m{}^7 u_m{}^8\rangle + \langle u_n{}^9 u_n{}^6 \,|\, u_m{}^7 u_m{}^8\rangle + \langle u_n{}^7 u_n{}^8 \,|\, u_m{}^6 u_m{}^8\rangle + \langle u_n{}^7 u_n{}^8 \,|\, u_m{}^6 u_m{}^9\rangle). \quad (38)$$

Only the two-center integrals were included in this calculation, using Hückel and Pariser wavefunctions. The results thus obtained are displayed in Table V. As in the case of the first-order theory, the contribution of the higher multipoles was estimated by evaluating the contribution of the dipole–dipole terms only, scaling this dipole term by the ratios between the calculated and experimental transition moment for the band (the transition moment for the β band is assumed to be correctly given by the theory), and subtracting the scaled dipole–dipole contribution from the total interaction energy. The contribution of the higher multipoles is of the order of 25% of the total interaction energy within the 50-Å sphere.

[15] D. P. Craig, J. Chem. Soc. **1955**, 2302.

TABLE V. Short-range configuration-interaction matrix elements for crystal-field p–β mixing in anthracene crystal (all energies in cm^{-1}).

	Translationally inequivalent molecules			Translationally equivalent molecules		
R	I_{dd}	HU	PA	I_{dd}	HU	PA
20	−1685	−1815	−1862	−386	−168.2	−197
25	−1667	−1774	−1825	−425	−263.6	−288
30	−1615	−1648	−1705	−461	−355	−371
35	−1612	−1638	−1697	−441	−304	−324
40	−1610	−1645	−1702	−467	−372	−387
45	−1620	−1665	−1722	−506	−470	−479
50	−1638	−1701	−1752	−536	−540	−545
55	−1650	−1725	−1779	−553	−581	−585
60	−1661	−1755	−1807	−561	−600	−600
65	−1670	−1775	−1826	−570	−620	−621
No. of cells						
2	−1835	−1760	−1805	−832	−1095	−1064
3	−1730	−1600	−1659	−775	−712	−705
4	−1627	−1667	−1717	−624	−636	−636
5	−1657	−1751	−1800	−594	−706	−712
6	−1669	−1781	−1828	−577	−622	−622
7	−1672	−1790	−1837	−571	−640	−639
8	−1675	−1790	−1837	−575	−628	−625

The corrected total interaction energy within this inner zone was obtained by multiplying the HU and PA terms in Table V by the scaling factors involving the squares of the calculated and experimental oscillator strengths for the p band, i.e., $(0.5/0.1)^{\frac{1}{3}}$ and $(0.38/0.1)^{\frac{1}{3}}$, respectively. For the region outside the 50-Å sphere, it was assumed that convergence of the higher-multipole interaction had been achieved, and only dipole–dipole terms remained to be summed from 50 Å to infinity. This summation was carried out using the continuum model.

We consider a cubic crystal with the same unit-cell volume as the aromatic monoclinic crystal and containing one dipole per unit cell. The formulas derived for the case of the infinite spherical crystal are now applicable. The contribution of the long-range dipole–dipole interactions to $\Gamma_{n1,mi}{}^{p\beta}$ involve the interaction between the transition dipole to the p state on one molecule and a β-state transition moment for another molecule and vice versa. For the calculation of the interaction between translationally equivalent molecules, we consider the fictitious dipole

$$\mathfrak{y}_n = 1/\sqrt{2}(\mathbf{p}_{n1}{}^{p} + \mathbf{p}_{n1}{}^{\beta}), \tag{39}$$

where $\mathbf{p}_{n1}{}^{p}$ and $\mathbf{p}_{n1}{}^{\beta}$ are the transition dipole moments to the p and β states on Molecule $n1$. Then the interaction between the dipole $\mathfrak{y}_n$ located at the origin and a set of parallel dipoles $\mathfrak{y}_m$ each located in the mth unit cell is

$$E(\mathfrak{y}_n, \mathfrak{y}_m) = \tfrac{1}{2}[E(\mathbf{p}_{n1}{}^{p}, \mathbf{p}_{m1}{}^{p}) + E(\mathbf{p}_{n1}{}^{\beta}, \mathbf{p}_{m1}{}^{\beta}) + E(\mathbf{p}_{n1}{}^{p}, \mathbf{p}_{m1}{}^{\beta}) + E(\mathbf{p}_{m1}{}^{\beta}, \mathbf{p}_{n1}{}^{p})], \tag{40}$$

where $E(\mathbf{p}_{n1}{}^{p}, \mathbf{p}_{m1}{}^{\beta})$ represents the interaction energy between a p-state transition moment of the reference molecule $n1$ and the β-state transition moments on all the translationally equivalent molecules. The calculation is straightforward, and, using the data in Table IV, we find

$$\tfrac{1}{2}[E(\mathbf{p}_{n1}{}^{p}, \mathbf{p}_{m1}{}^{\beta}) + E(\mathbf{p}_{n1}{}^{\beta}, \mathbf{p}_{m1}{}^{p})] = -1145 \text{ cm}^{-1}.$$

For the sum over translationally inequivalent molecules we take

$$\mathfrak{y}_n{}' = 1/\sqrt{2}(\mathbf{p}_{n2}{}^{p} + \mathbf{p}_{n1}{}^{\beta}). \tag{41}$$

The interaction energy between $\mathfrak{y}_n{}'$ at the origin and all the $\mathfrak{y}_m{}'$ dipoles in the fictitious crystal gives

$$E(\mathfrak{y}_n{}', \mathfrak{y}_m{}') = \tfrac{1}{2}[E(\mathbf{p}_{n1}{}^{\beta}, \mathbf{p}_{m1}{}^{\beta}) + E(\mathbf{p}_{n2}{}^{p}, \mathbf{p}_{m2}{}^{p}) + E(\mathbf{p}_{n1}{}^{\beta}, \mathbf{p}_{m2}{}^{p}) + E(\mathbf{p}_{n1}{}^{p}, \mathbf{p}_{n1}{}^{\beta})], \tag{42}$$

leading to $\tfrac{1}{2}[E(\mathbf{p}_{n1}{}^{\beta}, \mathbf{p}_{m2}{}^{p}) + E(\mathbf{p}_{n1}{}^{p}, \mathbf{p}_{m2}{}^{\beta})] = -847 \text{ cm}^{-1}$.

In Table VI we compare the total contribution of the dipole–dipole terms obtained by direct summation up to 50 Å and use of the continuum approximation for the outer region with the results of Fox and Yatsiv[7] who employed the Ewald method for evaluating the dipole sums. The agreement is good, lending support to the

TABLE VI. Contribution of dipole–dipole interaction terms to the matrix elements in the anthracene crystal.

Matrix element	This work (cm^{-1})		Fox and Yatsiv[a] (cm^{-1})	
	A_u	B_u	A_u	B_u
pp	−1120	−291	−920	−270
$\beta\beta$	−3578	29 094	−3500	25 000
$p\beta$	900	−4500	1140	4600

[a] These values are approximate since Fox and Yatsiv (Ref. 7) did not explicitly report the quantities tabulated: the entries have been inferred from their tables.

TABLE VII. First- and second-order interaction matrix elements for the p and β bands in anthracene (all quantities in cm^{-1}).

Int. to 55-Å sphere:	
$pp \sum_{\text{equiv}} = -340$	$pp \sum_{\text{inequiv}} = +16$
$\beta\beta \sum_{\text{equiv}} = +5800$	$\beta\beta \sum_{\text{inequiv}} = +10430$
$p\beta \sum_{\text{equiv}} = -265$	$\beta\beta \sum_{\text{inequiv}} = -790$
DD to 55-Å sphere:	
$pp \sum_{\text{equiv}} = -457$	$pp \sum_{\text{inequiv}} = +100$
$\beta\beta \sum_{\text{equiv}} = +6323$	$\beta\beta \sum_{\text{inequiv}} = +9736$
$p\beta \sum_{\text{equiv}} = -553$	$p\beta \sum_{\text{inequiv}} = -1650$
DD 55 Å:	
$pp \sum_{\text{equiv}} = -250$	$pp \sum_{\text{inequiv}} = 316$
$\beta\beta \sum_{\text{equiv}} = 6435$	$\beta\beta \sum_{\text{inequiv}} = 6600$
$p\beta \sum_{\text{equiv}} = -1145$	$p\beta \sum_{\text{inequiv}} = -840$

applicability of the continuum model to the calculation of long-range interactions in a monoclinic crystal containing more than one molecule per unit cell.

VI. NUMERICAL CALCULATIONS AND RESULTS

In Table VII we present the interaction matrix elements required for the computation of first- and second-order Davydov splittings in the p and β bands in anthracene. These results differ considerably from the dipole–dipole terms given in Table VI, thus demonstrating the importance of inclusion of the higher multipole terms. In Table VIII we list the various contributions to the first-order Davydov splitting in anthracene, again demonstrating the importance of higher multipoles and of long-range dipole–dipole interactions. On the other hand, the contribution of the electronic-exchange interaction K_{nm} in the anthracene p band is relatively small, in contrast with a previous conjecture[16] regarding the importance of electron-exchange terms for singlet-state Davydov splittings. The effect of the crystal-field mixing between the p and β states is readily obtained by diagonalization of the matrices

$$(A_u) = \begin{pmatrix} -922 & 251 \\ 251 & \Delta\omega - 4995 \end{pmatrix}$$

$$(B_u) = \begin{pmatrix} -258 & -3544 \\ -3544 & \Delta\omega + 29\,265 \end{pmatrix},$$

where $\Delta\omega = 14\,000\ cm^{-1}$ is the energy difference between the p and β states in the isolated molecule. The resulting energy levels corresponding to the p state are $-929\ cm^{-1}$ (for A_u) and $-560\ cm^{-1}$ (for B_u), while for the β band we find $9341\ cm^{-1}$ (for A_u) and $43\,836\ cm^{-1}$ (for B_u).

Throughout the previous discussion we have assumed that the Davydov splitting is large relative to the vibrational spacing. In this strong coupling limit, the wavefunction is represented by the product of the excited-state electronic wavefunction[3] and the ground-state vibrational wavefunction. In the weak coupling limit, the Davydov splitting is small compared to the vibrational spacing, and, instead of starting with the total electronic wavefunction, a different formalism must be used. (In the strong coupling limit, the vibrational part of the Hamiltonian is diagonalized after the crystal-field part; in the weak coupling case, the reverse order is taken.) In the weak coupling limit the molecular wavefunctions are constructed from vibronic functions, i.e.,[17]

$$\varphi_n^{f(i)} = \varphi_n^f \chi_n^{f(i)}, \tag{43}$$

where $\chi_n^{f(i)}$ is a vibrational wavefunction for the nth excited molecule in the ith vibrational state. When the functions defined by Eq. (43) are used as the basis for calculating the matrix elements of the intermolecular potential, the integrals are all modified as follows:

$$\langle \varphi_n^{f(i)} \varphi_m^0 \mid V_{nm} \mid \varphi_n^0 \varphi_m^{f(j)} \rangle = J_{nm} \langle \chi_n^{0(0)} \mid \chi_n^{f(i)} \rangle \langle \chi_m^{0(0)} \mid \chi_m^{f(j)} \rangle. \tag{44}$$

Therefore, in the weak-coupling limit, the total electronic matrix element is modified by vibrational overlap factors. It should be noted that in this case off-diagonal matrix elements between vibronic states corresponding

TABLE VIII. Davydov splittings in crystalline anthracene.

	Theory (cm^{-1})	Experiment (cm^{-1})
p band		
Dipole terms to 55 Å	+200	
Higher multipoles	−180	
Long-range dipole terms (from 55 Å to infinity)	+632	
Electron exchange	+30	
First-order splitting	622	
Second-order splitting (β state included)	350	450[a], 400[b]
β band		
First-order splitting	33 800	
Second-order splitting	34 495	(15 000)

[a] Reference 20.
[b] Reference 4.

[16] H. Sternlicht, G. C. Nieman, and G. W. Robinson, J. Chem. Phys. **38**, 1326 (1963).

[17] (a) W. T. Simpson and D. L. Peterson, J. Chem. Phys. **26**, 588 (1957); (b) A. Witkowski and W. Moffitt, *ibid.* **33**, 872 (1960).

TABLE IX. Davydov splittings in vibronic components of p state (assuming strong coupling in all other states).

	Calculated								Experimental	
	Only β state in configuration interaction				All π states in configuration interaction					
Band	$A_u(\|\|b)$	$B_u(\perp b)$	Δ	$P(b/a)$	$A_u(\|\|b)$	$B_u(\perp b)$	Δ	$P(b/a)$	Δ[a]	$P(b/a)$[b]
0-0	−404	−219	185	2.5	−437	−230	207	3.5	220(191)	5
0-1	1143	1228	85	1.6	1119	1221	102	2.5	141(150)	4.5
0-2	2640	2690	50	0.5	2632	2686	54	1.9	58(80)	3
0-3	4133	4153	20	...	4130	4152	22	...	...	...
0-4	5563	5573	10	...	5560	5573	13	...	...	...

[a] First set of data from Ref. 20; data in parentheses from Ref. 5.
[b] Reference 20.

to the same electronic transition must be included. If these off-diagonal terms are neglected, the vibrational sum rule $\sum_i |\langle\chi^{0(0)}|\chi^{f(i)}\rangle|^2=1$ implies that the total first-order electronic contribution to the Davydov splitting can be approximated by summation over all the experimental splittings corresponding to the individual vibronic components.

Since the total calculated splitting in the p state of anthracene is of the order of 500 cm^{-1} compared with a (symmetric) vibrational spacing of the order of 1400 cm^{-1}, we shall examine the theoretical predictions in the weak coupling limit. On the other hand, for the β band, an application of the strong coupling scheme seems more appropriate. For the computation of the Davydov splittings in the vibronic components of the band, we have considered four vibrational states with the diagonal and off-diagonal matrix elements given by (33). The configuration-interaction crystal-field-mixing matrix elements between the vibronic components of the p band and the β band are given by $\Gamma_{nm}{}^{p\beta}\langle\chi^{0(0)}|\chi^{p(i)}\rangle$.

The vibrational overlap integrals $\langle\chi^{0(0)}|\chi^{p(i)}\rangle$ can be obtained from the squares of the relative intensities (normalized to unity) of the vibronic components in the solution spectra. Alternatively, the Ross–McCoy[18] procedure for the evaluation of these overlap integrals may be employed. Using the procedure described in a previous paper,[12] we get, from the calculated bond-order changes,

$$\langle\chi^{0(0)}|\chi^{p(1)}\rangle=0.515(\text{exptl.}=0.570),$$
$$\langle\chi^{0(0)}|\chi^{p(2)}\rangle=0.590(\text{exptl.}=0.562),$$
$$\langle\chi^{0(0)}|\chi^{p(3)}\rangle=0.483(\text{exptl.}=0.466).$$

The 5×5 matrices were diagonalized, leading to the results displayed in Table VIII.

It is well known that a small amount of configuration mixing can lead to profound changes in the spectrum: our calculations for anthracene can therefore be further tested by examining the polarization ratios of the components of the $^1B_{2u}$ vibronic states. Let $\mathbf{M}^-$ and $\mathbf{M}^+$ be the transition moments parallel and perpendicular to the $\mathbf{b}$ axis. Then

$$\mathbf{M}^{\pm}=1/\sqrt{2}[(\mathbf{p}_1{}^{p^i}\pm\mathbf{p}_2{}^{p^i})+\lambda^{\pm}(p_i\beta)(\mathbf{p}_1{}^{\beta}\pm\mathbf{p}_2{}^{\beta})]. \quad (45)$$

In Eq. (34), $\lambda^{\pm}(p_i\beta)$ are the mixing coefficients between the vibronic component p_i and the β state, the superscripts p_i and β also referring to the same states. The polarization ratios

$$P(b/a)=[(\mathbf{M}^-\cdot\mathbf{b})/(\mathbf{M}^+\cdot\mathbf{a})]^2=[|\mathbf{M}|/(\mathbf{M}^+\cdot\mathbf{a})]^2 \quad (46)$$

are displayed in Table IX.

A crystal-field-mixing scheme involving only the p and β states is not complete; higher excited states must also be included. In order to take into account the effect of higher π-excited states in anthracene, the following procedure was employed. Pariser's[10] values of the energy levels of the π states having nonzero oscillator strength (i.e., a $^1B_{2u}$ state at 5.251 eV with oscillator strength of 0.091, a $^1B_{2u}$ state at 6.586 eV with oscillator strength of 0.644, and a $^1B_{3u}$ state at 7.221 eV with oscillator strength 0.091) were used. Since there is no $^1B_{2u}$ state at 5.251 eV in the solution spectrum,[19] but there is one at 5.65 eV, we arbitrarily added 0.4 eV to Pariser's energy values. Then, dipole sums for these levels were calculated using Pariser's oscillator strengths; the results were scaled by a factor arrived at in the following way: the dipole sums of the short-axis polarized ($^1B_{2u}$) states were scaled by the ratio of the experimental oscillator strength of the p band (also short-axis polarized) to the oscillator strength calculated by Pariser for the p band. The long-axis state ($^1B_{3u}$) sums were scaled by a similar ratio for the β state. The resulting 9×9 matrices (five vibronic components of the p and the β states, two $^1B_{2u}$, $^1B_{3u}$ states in the strong coupling limit, i.e., all intensity in the 0-0 band) are in Table X. The results for the splitting and the polarization ratio for the p band found by diagonalization of the above matrices are listed in Table IX (along with those results found by excluding the higher states). There is little difference in splittings, but the polarization ratios are considerably affected by including higher excited states.

[18] E. F. McCoy and I. G. Ross, Australian J. Chem. **4**, 573 (1962).

[19] L. E. Lyons and J. Morris, J. Chem. Soc. **1959**, 1551.

TABLE X. Configuration-interaction matrix elements for anthracene including five $\pi \rightarrow \pi^*$ excited states.

$^1B_{2u}(p)$					$^1B_{3u}(\beta)$	$^1B_{2u}$	$^1B_{2u}'$	$^1B_{3u}$
				(a) $A_u(\|\|b)$				
−300	−295	−246	−160	−118	142	−254	−680	−24
	1109	−242	−158	−116	141	−250	−669	−24
		2598	−132	−97	117	−208	−557	−20
			4114	−63	76	−136	−363	−13
				5554	56	−100	−267	−9
					9 365	122	325	−780
						19 800	−575	20
							28 500	50
								35 870
				(b) $B_u(\perp b)$				
−84	−83	−69	−45	−33	−2 077	−72	−191	−348
	1319	−68	−44	−32	−2 048	−71	−188	−343
		2743	−36	−27	−1 705	−59	−157	−285
			4176	−18	−1 111	−38	−102	−186
				5587	−816	−28	−75	−137
					43 535	−1 760	−4 700	4 950
						19 940	−170	−300
							29 570	−790
								36 825

VII. COMPARISON WITH EXPERIMENT

The experimental value of the Davydov splitting in the anthracene $^1A_{1g} \rightarrow {}^1B_{2u}$ band has only recently been established. Due to the width of the absorption bands, the positions of the bands and the Davydov splittings were found to depend on the thickness of the crystal unless very pure polarized light was used. The splitting in the 0–0 band has been reported to be 220 cm^{-1} by Brodin and Marisova,[20] 200 cm^{-1} by Wolf,[21] 190 cm^{-1} by Claxton *et al.*,[4] and 336 cm^{-1} by Lacey and Lyons.[22] Brodin and Marisova[20] report a total splitting (sum of all the vibronic components) in the p band of 450 cm^{-1} and Claxton *et al.*[4] have reported other measurements of this splitting in the vicinity of 400 cm^{-1}. An examination of Table VIII shows satisfactory agreement between our calculations and experiment.

In the anthracene β band, Craig[15] reports the component perpendicular to **b** to lie 10 000 cm^{-1} above the vapor transition and the component parallel to **b** to lie 5300 cm^{-1} below the vapor transition. The shift of the perpendicular component is so large that the transition lies in the vacuum-ultraviolet region and the exact position of the maximum is uncertain. (The bandwidth is very large.) Examination of Table VIII shows that the observed shift of the parallel component agrees with our calculation; the sign and magnitude of the shift of the perpendicular component also agrees, but the experimental data do not permit of quantitative comparison.

In Table IX we also compare the calculated and experimental splittings of the vibronic components of the p band with the available experimental data. The agreement regarding the sign and magnitude of the Davydov splitting is as good as can be expected.

The experimental intensity ratios of these individual vibronic components reveal a marked deviation from the oriented gas value $[P(b/a)=7.7]$ and show a definite trend, which is reproduced by our calculations when crystal-field mixing is taken into account. When only the effect of the β band is considered, the quantitative agreement is poor. Mixing higher excited states shows that there is a little difference in the splittings, but the polarization ratios are altered to be far closer to experiment.

VIII. EFFECT OF CRYSTAL SIZE ON THE DAVYDOV SPLITTING

The calculations described in the preceding sections were performed for a crystal of infinite size. In order to make a meaningful comparison between theory and experiment, the effect of the finite size of the crystal on the Davydov splitting must be considered. That the finite size of the crystal may be of considerable importance is suggested by the substantial contribution of long-range dipole–dipole interactions to the first- and second-order splittings. Experimental measurements usually refer to the splitting in crystals which are 0.1 μ thick and about 1 cm in diameter, with the wave vector of light in the crystal **c′** direction (i.e., **k** perpendicular to the *ab* crystal cleavage plane).

It is quite simple to consider the effect of the crystal on the Davydov splitting for a spherical crystal of radius R in the same approximation as defined by Eq. (31). Using the results described in Sec. IV and Appendix II, the dipole sum for the finite spherical crystal is related to the infinite crystal dipole sum by

$$I_{dd}(\text{finite}) = I_{dd}(\text{infinite})\{1-[3j_1(kR)/kR]\}, \quad (47)$$

[20] M. S. Brodin and S. V. Marisova, Opt. Spectry. **10**, 242 (1961) [Opt. i Spektroskopiya **10**, 473 (1961)].
[21] H. C. Wolf, Solid State Phys. **9**, 1 (1959).
[22] A. R. Lacey and L. E. Lyons, Proc. Chem. Soc. **1960**, 414.

where $j_1(x)$ is the spherical Bessel function of first order. It is worthwhile to notice that the finite lattice sum goes to zero for $\mathbf{k}\to\mathbf{0}$ and shows a rapid variation in the region $0<kR\leq 5$, converging for $kR\sim 10$ to the infinite sphere result. Since for our case $\mathbf{k}\sim 2\times 10^{+5}$ cm^{-1} (which is of the order of the reciprocal of the crystal thickness used in the actual experiments), the contribution of the long-range dipole–dipole terms should depend on the crystal thickness. However, the spherical crystal is not a good representation of the actual physical case, and we shall demonstrate that, under the experimental conditions actually employed, the Davydov splitting is expected to be independent of the crystal thickness.

We turn our attention to a cylindrical crystal. This is, in fact, a faithful representation of the actual case. Since $\mathbf{k}\neq\mathbf{0}$ the dipole sum converges to a value independent of the crystal shape, so that the dipole sum for the infinite cylinder is equal to that for the infinite sphere.

As in the case previously considered, we assume that the interactions within a region of exclusion are to be directly summed. This exclusion region now consists of a cylindrical volume of radius ρ_0 and height a around the origin. For the outer region we again consider a lattice of parallel dipoles with one dipole per unit volume and replace the lattice sum by an integral

$$I_{dd}=\sum_{R_i}\exp(i\mathbf{k}\cdot\mathbf{R}_i)\left[\frac{1-3\cos^2(\mathfrak{y}\cdot\mathbf{R}_i)}{R_i^3}\right]$$
$$\to V_0^{-1}\int d\mathbf{R}\exp(i\mathbf{k}\cdot\mathbf{R})\left[\frac{1-3\cos^2(\mathfrak{y}\cdot\mathbf{R})}{R^3}\right], \quad (48)$$

where the integral is taken outside the excluded volume. This integral may be broken into three parts:

(1) The annulus of inner radius ρ_0, outer radius L, and height a, leading to a contribution I_1.

(2) The cylinder of radius L and height $M-(a/2)$. This cylinder, above the annulus, leads to a contribution of I_2.

(3) The cylinder below the annular region of the same dimension as (2). By direct summation $I_{dd}=I_1+2I_2$.

At this point it should be mentioned that in the experiments reported, $L\sim 1$ cm, while $a\sim 10^{-5}$ cm. As shown in Appendix III,

$$I_1=\frac{4\pi}{V_0}P_2[\cos(\mathfrak{y}\cdot\mathbf{k})]\int_0^{a/2}dz\exp(i\,|\,\mathbf{k}\,|\,z)$$
$$\times\left[\frac{\rho_0^2}{(\rho_0^2+z^2)^{\frac{3}{2}}}-\frac{L^2}{(L^2+z^2)^{\frac{3}{2}}}\right]. \quad (49)$$

Then, as $L\to\infty$ (i.e., $L/a\to 10^5$), we get

$$I_1=\frac{4\pi}{V_0}P_2(\cos\mathfrak{y}\cdot\mathbf{k})\int_0^{a/2}dz\frac{\rho_0^2\exp(i\,|\,\mathbf{k}\,|\,z)}{(\rho_0^2+z^2)^{\frac{3}{2}}}. \quad (50)$$

Consider now the second contribution:

$$I_2=-\frac{4\pi}{V_0L}P_2(\cos\mathfrak{y}\cdot\mathbf{k})\int_{a/2}^{M}dz\frac{\exp(i\,|\,\mathbf{k}\,|\,z)}{(1+z^2/L^2)^{\frac{3}{2}}}. \quad (51)$$

For a finite value of $\mathbf{k}$, when $L\to\infty$, $I_2\to 0$.[23] Thus we have shown[24] that the entire contribution to the dipole sum for a cylindrical crystal with $\mathbf{k}$ perpendicular to the plane face of the cylinder arises from the annular region and the excluded inner zone. This result may be justified by the following intuitive argument: Consider an infinitely wide and infinitely thin plate of dipoles above the test dipole, which is not in the plate. Let us consider two cases: (a) All the dipoles are perpendicular to the plate; the plate then acts as a condenser, and since the field is zero outside a condenser, there is no interaction between the dipoles in the plate and the test dipole; (b) all the dipoles are parallel to the plate; then the field due to the dipoles in the plate has a discontinuity at infinity, and there is no interaction between the dipoles within the plate and the test dipole. Hence, for any orientation of dipoles, an infinitely thin and infinitely wide plate does not interact with a dipole outside. Of course, for a finite thickness, the modulation of the dipoles by the $\exp(i\mathbf{k}\cdot\mathbf{R})$ terms has to be included. However, we have shown that for $\mathbf{k}$ perpendicular to the plane there is no contribution outside the annular region.

For the case of a real aromatic crystal, the thickness of the annular region is determined by the distance where the continuum approximation involving the construction of effective unit-cell dipoles is applicable. As shown in Sec. IV, a value of $a\approx 50$ Å is suitable. Hence we conclude that, under any experimental conditions when $\mathbf{k}\,||\,(\mathbf{c}')^{-1}$, the entire long-range contribution to the Davydov splitting will arise from the annular region, and the experimental splitting should be independent of the crystal thickness. It is worth mentioning that Brodin and Marisova[20] found no systematic change in the factor-group splitting in the p state of anthracene varying the crystal width in the region 0.05–0.1 μ.

The results just obtained imply that, under the conditions discussed above, the region of coherent excitation in the crystal is not limited by the crystal thickness, as long as the crystal width (i.e., area) is infinite. Under the experimental conditions usually employed, the size of the exciton packet is determined by the reciprocal of the absorption coefficient and by the infinite width of the crystal. Although the change of phase across the exciton packet in the $\mathbf{k}$ direction is relatively small (i.e., $kR\sim 1$, the absorption coeffi-

[23] It is worthwhile noting at this point that for $\mathbf{k}=\mathbf{0}$, I_{dd} depends on the ratio M/L, i.e., the shape of the cylinder.

[24] The same result can be obtained by maximizing the integral I_2, so that

$$I_2(\max.)=-\frac{4\pi}{N_0}\frac{L^2}{(L^2+a^2/4)^{\frac{3}{2}}}\int_{a/2}^{M}\exp(i\,|\,\mathbf{k}\,|\,z)dz.$$

As the integral on the right is finite for all values of M, then for large L, $I_2(\max.)\to 0$.

cients are of the order of 10^5–10^6 cm^{-1} in aromatic crystals), size effects are not expected because of the infinite crystal width. Moreover, as long as $\mathbf{k}$ is in the $\mathbf{c}'$ direction, the energy of the two Davydov components will be independent of the crystal shape. Finally, no size effects are expected to contribute to the absorption bands.

Before closing this discussion, it is worth mentioning that, if $\mathbf{k}$ is not perpendicular to the *ab* plane of the cylindrical crystal, size effects on the splitting would be expected to show up, depending on the angle between $\mathbf{k}$ and $(\mathbf{c}')^{-1}$.

IX. EFFECT OF CHARGE-TRANSFER STATES

Up to this point we have followed the formulation of exciton theory within the framework of the tight binding approximation, constructing zero-order crystal wavefunctions based on the free-molecule wavefunctions. Recently, the simple exciton theory was extended to include charge-transfer (ion-pair) exciton states constructed by removing an electron from one molecule and locating it on another molecule in the crystal.[12] Ion-pair exciton states are expected to make a considerable contribution to neutral exciton states characterized by a relatively small bandwidth, i.e., neutral-triplet exciton states and neutral-singlet exciton states corresponding to very weak molecular transitions. In the analysis cited, the crystal wavefunctions and the energy levels for charge-transfer exciton states were derived, and configuration interaction between charge-transfer and neutral-triplet exciton states was examined. It is also interesting to examine the configuration interaction between charge-transfer states and neutral-singlet exciton states arising from a relatively weak molecular transition, e.g., the anthracene p band. Since the interaction is short range, we need only consider ion-pair functions where the positive and negative ions are near neighbors. As before, the matrix elements connecting the neutral and charge-transfer exciton states can be expressed in the form:

$$B(i,j)=\langle R_i \mid H \mid R_i,\ R_j\rangle-\langle R_i \mid R_iR_j\rangle\langle R_i \mid H \mid R_i\rangle$$

and

$$C(i,j)=\langle R_i \mid H \mid R_j,\ R_i\rangle-\langle R_i \mid R_jR_i\rangle\langle R_i \mid H \mid R_i\rangle, \tag{52}$$

where $\mid R_i\rangle$ refers to a localized excitation on Molecule i, while $\mid R_i,\ R_j\rangle$ is the ion-pair wavefunction where the positive and negative charges are located on Molecules i and j, respectively.

Considering only matrix elements where the molecular excitation and the negative (or positive) ion are located on the same molecule, it was previously shown that only the following eight ion-pair exciton wavefunctions, $E_1^{\mp}=\mid \mathbf{0},\ \boldsymbol{\tau};\ \mp\rangle$, $E_2^{\mp}=\mid \boldsymbol{\tau},\ \mathbf{0};\ \mp\rangle$, $E_3^{\mp}=\mid \mathbf{0},\ \mathbf{c}+\boldsymbol{\tau};\ \mp\rangle$, and $E_4^{\mp}=\mid \mathbf{c}+\boldsymbol{\tau},\ \mathbf{0};\ \mp\rangle$, have different mixing coefficients for the states of A_u and B_u symmetry, and only these states will contribute to the Davydov splitting. The configuration-interaction matrix elements take the form:

$$\begin{aligned}
K_1^{\mp}&=\langle E_1^{\mp} \mid H \mid E_1^{\mp}\rangle-\langle E_1^{\mp} \mid \Psi_{\mp}^{f}\rangle\langle\Psi_{\mp}^{f} \mid H \mid \Psi_{\mp}^{f}\rangle=\sqrt{2}[B(\mathbf{0},\boldsymbol{\tau})+B(\boldsymbol{\tau},\mathbf{0})\mp C(\mathbf{0},\boldsymbol{\tau})\mp C(\boldsymbol{\tau},\mathbf{0})],\\
K_2^{\mp}&=\sqrt{2}[C(\mathbf{0},\boldsymbol{\tau})+C(\boldsymbol{\tau},\mathbf{0})\mp B(\mathbf{0},\boldsymbol{\tau})\mp B(\boldsymbol{\tau},\mathbf{0})],\\
K_3^{\mp}&=\sqrt{2}[B(\mathbf{0},\mathbf{c}+\boldsymbol{\tau})+B(\mathbf{c}+\boldsymbol{\tau},\mathbf{0})\mp C(\mathbf{0},\mathbf{c}+\boldsymbol{\tau})\mp C(\mathbf{c}+\boldsymbol{\tau},\mathbf{0})],\\
K_4^{\mp}&=\sqrt{2}[C(\mathbf{0},\mathbf{c}+\boldsymbol{\tau})+C(\mathbf{c}+\boldsymbol{\tau},\mathbf{0})\mp B(\mathbf{0},\mathbf{c}+\boldsymbol{\tau})\mp B(\mathbf{c}+\boldsymbol{\tau},\mathbf{0})].
\end{aligned}\tag{53}$$

The matrix elements were evaluated by the methods described previously,[12] leading to the general results

$$\begin{aligned}
B(\mathrm{A},\mathrm{B})=&\langle u_A^8 \mid V_B^{GMS} \mid u_B^8\rangle-\langle u_A^8 \mid u_B^8\rangle\langle u_A^8 \mid V_B^{GMS}+2K_A^7-J_A^7 \mid u_A^8\rangle+\langle u_A^8 \mid K_A^7-\sum_{s=1}^{7}K_B^s \mid u_B^8\rangle\\
&-\langle u_A^8 \mid u_B^7\rangle\langle u_B^8 \mid V_A^{GMS} \mid u_B^7\rangle+\langle u_A^7 \mid u_B^8\rangle\langle u_A^7 \mid V_B^{GMS} \mid u_A^8\rangle+\langle u_A^8 \mid u_B^7\rangle\langle u_B^8u_B^7 \mid u_A^7u_A^7\rangle\\
&-\langle u_A^7 \mid u_B^7\rangle\langle u_A^7u_A^8 \mid u_B^7u_B^8\rangle-\sum_{i=1}^{6}(\langle u_A^i \mid u_B^8\rangle\langle u_A^i \mid V_B^{GMS} \mid u_A^8\rangle+\langle u_A^i \mid u_B^8\rangle\langle u_A^i \mid K_A^7-J_A^7 \mid u_A^8\rangle\\
&+\langle u_A^8 \mid u_B^i\rangle\langle u_B^i \mid V_A^{GMS}-J_A^7+K_B^7 \mid u_B^K\rangle-\langle u_A^7 \mid u_B^i\rangle\langle u_A^8u_A^7 \mid u_B^8u_B^i\rangle-\langle u_A^8 \mid u_B^8\rangle\langle u_A^8u_B^i \mid u_B^iu_B^K\rangle).
\end{aligned}\tag{54}$$

$$\begin{aligned}
C(\mathrm{A},\mathrm{B})=&-\langle u_B^7 \mid V_B^{GMS} \mid u_A^7\rangle+\sum_{i=1}^{7}\langle u_B^7 \mid K_B^s \mid u_A^7\rangle-\langle u_B^7u_A^7 \mid u_A^8u_A^8\rangle+\langle u_A^7 \mid u_B^7\rangle\langle u_B^7 \mid V_B^{GMS} \mid u_B^7\rangle\\
&+2\langle u_A^7 \mid K_A^8 \mid u_B^7\rangle+2\langle u_B^7 \mid u_B^8\rangle\langle u_A^8 \mid V_B^{GMS}-J_B^7 \mid u_A^7\rangle\\
&+\sum_{i=1}^{6}(\langle u_A^7 \mid u_B^i\rangle\langle u_B^7 \mid V_A^{GMS}+J_A^8-J_A^7 \mid u_B^i\rangle-\langle u_B^7 \mid u_A^7\rangle\langle u_A^7 \mid K_B^i\rangle+\langle u_B^7 \mid u_A^i\rangle\langle u_A^i \mid K_A^8 \mid u_A^7\rangle),
\end{aligned}\tag{55}$$

where V_A^{GMS} is the Goeppert-Mayer–Sklar potential of Molecule A, and J_A^i and K_A^i are the Coulomb and exchange operators of the orbitals u_A^i.

The configuration-interaction matrix elements are displayed in Table XI.

The energies of the charge-transfer states in anthracene were estimated from classical considerations.[12] The energies of the $E_1^{\mp}$ and $E_2^{\mp}$ states were found to be 3.4±0.5 eV, while the energies of the $E_3^{\mp}$ and $E_4^{\mp}$ states are 4.4±0.5 eV above the ground state. The difference between these energies arises from different Coulomb interactions in the states where the charges are located on **0** and τ or on **0** and **c**+τ, respectively. Since the energies of the charge-transfer states are expected to lie close to the p band (3.1 eV), perturbation theory is not applicable, and the 6×6 energy matrices (for the A_u and B_u states, separately) involving the p, β, and four charge-transfer states were diagonalized.[25] Moreover, since the location of the charge-transfer states is uncertain, we have used the energy difference between the p and the E_1 (or E_2) states as an adjustable parameter, while the energy difference between the E_1 and E_3 states is taken to be 1 eV. The results thus obtained are displayed in Fig. 1, where we have plotted the relative energies and the percentage of p in each of the components.

For a $p-E_1^{\mp}$ separation of -600 to $+400$ cm^{-1}, four bands in the absorption spectrum are expected, two **b** polarized and two polarized in the *ac* plane. It should be noted that the intrinsic intensity of the transition to the charge-transfer states is expected to be small (characterized by an oscillator strength of the order of $f=10^{-5}$–10^{-6}), and such transitions may only be amenable to experimental observation in pure crystals when appreciable mixing with neutral-exciton states occurs. The available experimental data are not consistent with the above picture, as only one A_u and one B_u component are observed for each vibronic state. It is then necessary that the separation between the charge transfer and the p bands in crystal anthracene be larger than 500 cm^{-1}. Under these conditions, the effect of charge-transfer states on the p-band splitting is small (Fig. 1). The experimental observations,[5,20] therefore, do not yield evidence regarding the location of the first charge-transfer states E_1 and E_2 in this system. In addition, recent experimental observations on thick (1 cm) anthracene crystals[26] also fail to yield any evidence for the location of the charge-transfer state on the low-energy tail of the band in anthracene. It is conceivable that these states are located somewhere between the p and β neutral-exciton states of the crystal.

TABLE XI. B and C coefficients for $^1B_{2u}(p)$ anthracene (all energies in units of 10^{-2} electron volts).

i	j	$B(i,j)$	$C(i,j)$
0	τ	1.96	0.547
0	**c**+τ	−0.508	2.65
τ	**0**	1.90	0.435
c+τ	**0**	−0.478	2.65

X. DISCUSSION

In the work presented herein, a detailed study is made of the lower excited states of a typical aromatic crystal. It is shown that calculations of the magnitudes and signs of the Davydov splittings and the intensity and polarization ratios of the vibronic components of the transition to the lowest excited state of anthracene are in satisfactory agreement with experiment. It is somewhat disappointing that, despite considerable progress in the understanding of the excited states of π-electron systems, the available wavefunctions are not of sufficient accuracy to permit *a priori* calculations of the properties of singlet-exciton states. The criterion for the accuracy of the molecular wavefunction employed herein is the set of magnitudes of the oscillator strengths predicted for the free-molecule transitions. In view of the serious overestimates of oscillator strengths, even when configuration-interaction molecular wavefunctions are employed, some scaling of the intermolecular Coulomb interaction integrals is necessary. It is interesting to note at this point that the electron-exchange intermolecular integrals, which contribute only a small correction term in the case of singlet-exciton states, are not markedly affected by the molecular functions employed. For the naphthalene triplet state, it was found that the Pariser wavefunction leads to a triplet-state Davydov splitting which is only 10% lower than that obtained by using the Hückel function.

It is pertinent to consider again the importance of the various contributions to the energies of singlet exciton states in aromatic molecular crystals:

(a) The problem of calculating energies in molecular crystals cannot be reduced to the summation of dipole–

[25] The off-diagonal matrix element between neutral and charge-transfer states may be derived by considering a set of wavefunctions Φ_i characterized by extremely small overlap. In this case, the symmetric orthogonalization procedure [P.-O. Löwdin, J. Chem. Phys. **18**, 365 (1950)] is applicable:

$$\Phi_i' = \Phi_i - \tfrac{1}{2}\sum_d \Phi_j S_{ji} + \tfrac{3}{8}\sum_{k,l} \Phi_k S_{kl} S_{li} - \cdots,$$

where

$$S_{kl} = \langle \Phi_k \mid \Phi_l \rangle - \delta_{kl}.$$

Thus

$$H_{ik}' = H_{ik} - \tfrac{1}{2}\sum_d (S_{ij}H_{jk} + H_{ij}S_{jk}) + \cdots,$$

and, since the overlaps are so small, we may neglect higher-order terms in S. Then, if our Hamiltonian has off-diagonal matrix elements much smaller than the diagonal elements,

$$H_{ik}' = H_{ik} - S_{ik}H_{kk} + \tfrac{1}{2}S_{ik}(H_{kk} - H_{ii}),$$

and we may neglect the last term for the cases we consider here. Thus the off-diagonal matrix elements are given by $K_i^{\mp}$.

[26] R. S. Berry, J. Jortner, J. C. Mackie, E. Pysh, and S. A. Rice, J. Chem. Phys. **42**, 1535 (1965).

dipole interactions. From π-electron theory, it has been demonstrated that short-range higher-multipole interactions yield important contributions to the diagonal and off-diagonal matrix elements. The most striking case is that of the diagonal terms for the p state, where the higher multipoles reduce the contribution within the sphere of 50 Å from 100 cm^{-1} for dipole–dipole terms to 16 cm^{-1}. The importance of higher multipole interactions has been pointed out by Craig *et al.*[4] However, in their calculations the transition octopole moment (for $g \rightarrow u$ transitions) was used as an adjustable variable to obtain agreement with experiment.

(b) Electron-exchange interactions in the allowed singlet state ($^1B_{2u}$ in anthracene) were found to be small.

(c) The long-range dipole–dipole interactions are of great importance, and any meaningful theory of singlet-exciton states arising from allowed transitions must take the long range of the interaction into account.[27] The computation of this contribution is greatly facilitated by applying the continuum approximation used in this paper. Long-range interactions involving modulated dipole sums are absolutely convergent, and, under the experimental conditions employed to date, the Davydov splitting is predicted to be independent of the crystal thickness. The contribution of long-range retarded dipole terms has recently been studied by Simpson[28] using quantum electrodynamics. Simpson's analysis leads to the same formula as is obtained in Appendix II of this paper. Hall[29] and Amos[30] have shown that, when only dipole–dipole interactions are included in the lowest excited states of molecular crystals, the classical theory of long waves developed by Born and Huang[31] for vibrations of ionic crystals is applicable. These authors examined the coupling between electromagnetic waves and transverse-exciton waves and the set of dispersion relations obtained therefrom. The effect of higher excited states was included in terms of a frequency-independent polarizability term.

(d) In the analysis presented here, the effects of configuration interaction between singlet-exciton states have been carefully examined. It was found that the mixing between p and β singlet states has a large effect on the Davydov splitting, while inclusion of higher excited π states has only a minor effect on the splittings. However, to account for the polarization ratios in the vibronic components of the p band, higher excited states must be included.

(e) Charge-transfer exciton states were found to have only a small effect on the anthracene p-band Davydov splitting. It appears that the charge-transfer state will only slightly influence singlet-exciton states arising from allowed transitions (i.e., characterized by an oscillator strength higher than 0.01). On the other hand, these charge-transfer exciton states may appreciably affect singlet-exciton states arising from symmetry-forbidden vibronically induced transitions (i.e., the $^1B_{2u}$ state of benzene) or symmetry-allowed but mainly vibronically induced transitions [i.e., the $^1B_{3u}(\alpha)$ state of naphthalene].

For the case of naphthalene, the splitting in the 0–0 band of the α state is reported to be about 160 cm^{-1} with the component perpendicular to **b** lying lower than does the component parallel to **b**. From the analysis presented here, the contribution of two-center integrals will vanish, and the Davydov splitting is expected to be smaller than 10 cm^{-1}. This result is a consequence of the pairing property of Hückel or SCF π-electronic wavefunctions. Inclusion of intramolecular overlap in the Hückel wavefunctions destroys the pairing properties of the π orbitals, but the resultant splitting is small, and the components are inverted from what is found experimentally. Now, the pairing property of π-electron orbitals has been extensively tested by examination of the electron paramagnetic resonance spectra and optical spectra of positive and negative hydrocarbon ions. In all cases, it is found that the pairing of orbitals provides an accurate description of the observations. We therefore conclude that some other explanation than "poor wavefunctions" must be invoked to explain the observations. Recent work in this laboratory indicates that crystal-field mixing of ion-pair (charge-transfer) exciton states with the α state explains the observations. This work will be reported in a separate publication.

Aside from questions related to quantitative details, perhaps the most important deduction to be drawn from the work reported herein is that the observed spectra of aromatic crystals represent only the end effects of very subtle balances and interactions between all the states within the molecular electronic manifold. In this sense, then, the simplest version of exciton theory is an inadequate description of real systems.

ACKNOWLEDGMENTS

We are grateful to Dr. R. Pariser for sending us his unpublished SCF wavefunctions for anthracene. We wish to thank Professor M. H. Cohen, Dr. N. R. Kestner, and Mr. M. T. Vala, Jr., for many helpful discussions and Dr. J. L. Katz for his assistance in the evaluation of the molecular integrals. We also wish to thank the (anonymous) referee for stimulating comments on the retarded interaction.

This research was supported by the U.S. Public Health Service, the National Science Foundation, the Directorate of Chemical Sciences of the U.S. Air Force

[27] It should be noted that the conditional convergence of the dipole sum is characteristic of the three-dimensional crystal. For one-dimensional crystal models of physical interest, i.e., polymers, the dipole sum converges within a relatively small distance (~50 Å).

[28] W. T. Simpson, Radiation Res. **20**, 87 (1963).

[29] G. G. Hall, Proc. Roy. Soc. (London) **A270**, 285 (1962).

[30] A. T. Amos, Mol. Phys. **6**, 393 (1963).

[31] M. Born and K. Huang, *Dynamical Theory of Crystal Lattices* (Oxford University Press, New York, 1954).

Office of Scientific Research, and the Petroleum Research Fund of the American Chemical Society. We have also benefited from the use of facilities provided in part by the Advanced Research Projects Agency for materials research at the University of Chicago.

APPENDIX I: CALCULATION OF INTEGRALS

The Coulomb integrals are of the form

$$I=\langle u_n{}^i u_n{}^j \mid u_m{}^k u_m{}^l\rangle$$

$$=\int u_n{}^i(1)\,{}^*u_m{}^l(2)\,{}^*(r_{12}{}^{-1})\,u_n{}^j(1)\,u_m{}^k(2)\,d\tau_1 d\tau_2, \quad \text{(A1)}$$

where $u_n{}^i$ is the ith molecular orbital on the nth molecule. We may break this up into atomic integrals $(\omega_n{}^\alpha)$ to get

$$I=\sum_{\alpha,\beta,\gamma,\delta} c_\alpha{}^i c_\beta{}^j c_\gamma{}^k c_\delta{}^l(\omega_n{}^\alpha\omega_n{}^\beta/\omega_m{}^\gamma\omega_m{}^\delta), \quad \text{(A2)}$$

where α, β are atoms on Molecule n and γ, δ are atoms on Molecule m, and the c's are Hückel or SCF coefficients. If we consider only two-center terms, we find

$$I=\sum_{\alpha,\beta} c_\alpha{}^i c_\alpha{}^j c_\gamma{}^k c_\gamma{}^l(\omega_n{}^\alpha\omega_n{}^\alpha/\omega_m{}^\gamma\omega_m{}^\gamma). \quad \text{(A3)}$$

The SCF carbon-atom wavefunctions used in the computation of the integrals are a linear combination of four Slater orbitals characterized by the parameters[32]:

$$a_1=0.00842, \quad a_2=0.17442,$$
$$\alpha_1=6.827, \quad \alpha_2=2.779,$$
$$a_3=0.45191, \quad a_4=0.43645,$$
$$\alpha_3=1.625, \quad \alpha_4=1.154.$$

These atomic Coulomb integrals involve the interaction between $2p\pi$ orbitals at orientations determined by the crystal structure. The coordinate system used in this calculation is the same as that used by Kotani *et al.*[33] The line joining Atoms α and γ defines the z axis, and we may choose the y axis to be perpendicular to one orbital, defining

$$A=\mathbf{n}\cdot\mathbf{x}_\alpha, \quad B=\mathbf{n}\cdot\mathbf{y}_\alpha=0, \quad C=\mathbf{n}\cdot\mathbf{z}_\alpha,$$
$$D=\mathbf{m}\cdot\mathbf{x}_\gamma, \quad E=\mathbf{m}\cdot\mathbf{y}_\gamma, \quad F=\mathbf{m}\cdot\mathbf{z}_\gamma,$$

where $\mathbf{n}$ and $\mathbf{m}$ are unit vectors in the direction of the $2p\pi$ orbitals located on Centers α and γ, respectively. We find that the atomic Coulomb integrals may be expressed as

$$(\omega_n{}^\alpha\omega_n{}^\alpha \mid \omega_m{}^\gamma\omega_m{}^\gamma)=A^2(D^2+E^2)\,\langle p{+}p{+} \mid p{-}p{-}\rangle+(A^2/2)\,(D^2-E^2)\,\langle p{+}p{-} \mid p{-}p{+}\rangle+[A^2F^2+C^2(D^2+E^2)]$$
$$\times\langle pzpz \mid p{-}p{-}\rangle+4ACDF\,\langle p{+}pz \mid p{-}pz\rangle+C^2p^2\,\langle pzpz \mid pzpz\rangle. \quad \text{(A4)}$$

The exchange integrals may be written

$$I=\langle u_n{}^i u_m{}^k \mid u_n{}^j u_m{}^l\rangle$$
$$=\int u_n{}^i(1)\,{}^*u_m{}^l(2)\,{}^*r_{12}{}^{-1}u_n{}^j(2)\,u_m{}^k(1)\,d\tau_1 d\tau_2. \quad \text{(A5)}$$

These may be broken up into sums over atomic integrals and, if we only keep two-center terms, we get

$$I'=\sum_{\alpha,\beta} C_\alpha{}^i C_\alpha{}^j C_\beta{}^k C_\beta{}^l\,\langle\omega_n{}^\alpha\omega_m{}^\beta \mid \omega_n{}^\alpha\omega_m{}^\beta\rangle. \quad \text{(A6)}$$

The atomic integrals may be again broken up into a sum of basic integrals. Using the same definitions as above for A, B, C, D, E, F we get

$$\langle\omega_n{}^\alpha\omega_m{}^\beta \mid \omega_n{}^\alpha\omega_m{}^\beta\rangle=A^2D^2\,\langle p{+}p{+} \mid p{-}p{-}\rangle+A^2(D^2+E^2)\,\langle p{+}p{-} \mid p{-}p{+}\rangle+[A^2F^2+C^2(D^2+E^2)]$$
$$\times\langle p{+}pz \mid p{-}pz\rangle+2ACDF\,\langle p{+}pz \mid pzp{+}\rangle+2ACDF\,\langle p{+}p{-} \mid pzpz\rangle+C^2F^2\,\langle pzpz \mid pzpz\rangle. \quad \text{(A7)}$$

These atomic Coulomb and exchange integrals were calculated on an IBM 7094 computer using an integral program written by A. C. Wahl and P. E. Cade of the Laboratory of Molecular Structure and Spectra, the University of Chicago. The basic integrals are presented in Table XII.

APPENDIX II: DIPOLE–DIPOLE INTERACTIONS IN THE OUTER ZONE

In this appendix we evaluate the interaction between a dipole and the dipole field of all the matter in a spherical crystal, excluding a spherical inner zone. Since the convergence length is of the order of magnitude of k^{-1}, it is necessary to include the effects of retardation of the interaction potential. Following Anex and Simpson[34] or Born and Wolf,[35] we take for the field of

[32] P. Bagus, T. Gilbert, C. C. J. Roothaan, and H. D. Cohen, "Analytic SCF Functions for First Row-Atoms," (to be published).

[33] M. Kotani, E. Ishiguro, and K. Hijikata, J. Phys. Soc. Japan **9**, 553 (1954).

[34] A. I. Kitaigorodskii, *Organic Chemical Crystallography* (Consultants Bureau, New York, 1961).

[35] M. Born and H. C. Wolf, *Principles of Optics* (Pergamon Press, Ltd., London, 1959).

Table XII. Atomic Coulomb integrals (II/JJ). All quantities are in atomic units.

R	(P+P-/P-P+)	(P+P+/P+P+)	(PZP+/P+PZ)	(PZPZ/P+P+)	(PZPZ/PZPZ)
3.5	0.4031558E-02	0.2560267E-00	0.4996384E-02	0.2761665E-00	0.3246734E-00
4.0	0.2466467E-02	0.2294808E-00	0.3548337E-02	0.2456420E-00	0.2849084E-00
4.5	0.1532203E-02	0.2074731E-00	0.2452050E-02	0.2203102E-00	0.2512529E-00
6.0	0.4178764E-03	0.1584460E-00	0.7856429E-03	0.1649458E-00	0.1794615E-00
6.5	0.2844025E-03	0.1470952E-00	0.5474444E-03	0.1523696E-00	0.1638101E-00
7.0	0.1980794E-03	0.1372151E-00	0.3871139E-03	0.1415395E-00	0.1506577E-00
7.5	0.1409818E-03	0.1285457E-00	0.2781563E-03	0.1321270E-00	0.1394831E-00
8.0	0.1023739E-03	0.1208825E-00	0.2031538E-03	0.1238770E-00	0.1298843E-00
20.0	0.1051449E-05	0.4929078E-01	0.2102898E-05	0.4949906E-01	0.4985280E-01
26.0	0.2831875E-06	0.3797350E-01	0.5664237E-06	0.3806889E-01	0.3823154E-01
40.0	0.3286341E-07	0.2470228E-01	0.6606430E-07	0.2472860E-01	0.2482830E-01
45.0	0.1823925E-07	0.2194988E-01	0.3688721E-07	0.2196837E-01	0.2209270E-01
50.0	0.1077114E-07	0.1974204E-01	0.2196950E-07	0.1975552E-01	0.1991092E-01
60.0	0.4326504E-08	0.1642159E-01	0.8942082E-08	0.1642939E-01	0.1662360E-01

a small oscillating dipole $\boldsymbol{\mu}_i$:

$$\mathbf{E}_i=\boldsymbol{\mu}_i\cdot(k^2\mathbf{1}+\nabla\nabla)[\exp(ikR_i)/R_i]$$
$$=\exp(ikR_i)\left\{\frac{3(\boldsymbol{\mu}_i\cdot\mathbf{R}_i)\mathbf{R}_i-R_i^2\boldsymbol{\mu}_i}{R_i^5}(1-ikR_i)\right.$$
$$\left.-k^2\left[\frac{(\boldsymbol{\mu}_i\cdot\mathbf{R}_i)\mathbf{R}_i-R_i^2\boldsymbol{\mu}_i}{R_i^3}\right]\right\}. \quad \text{(A8)}$$

The energy of interaction between two such dipoles is $-\boldsymbol{\mu}_i\cdot\mathbf{E}_i$, and we must sum over all dipoles in the crystal. As noted in the main part of this paper, it is valid to replace the summation by an integration and represent the bulk of the crystal by a continuous dipole density. Now, (A8) has a real part and an imaginary part, which we take to be the energy and the damping, respectively. Converting to the integral representation,

$$E=\sum_i\boldsymbol{\mu}\cdot\mathbf{E}_i$$
$$=\frac{1}{V}\int\exp(i\mathbf{k}\cdot\mathbf{R})\left\{\frac{\mu^2R^2-3(\boldsymbol{\mu}\cdot\mathbf{R})^2}{R^5}(\cos kR+kR\sin kR)\right.$$
$$\left.+k^2\left(\frac{(\boldsymbol{\mu}\cdot\mathbf{R})^2-\mu^2R^2}{R^3}\right)\cos kR\right\}\sin\theta d\theta d\phi R^2dR. \quad \text{(A9)}$$

Let the z axis lie along $\mathbf{k}$, and set $\boldsymbol{\mu}\cdot\mathbf{y}=0$. These two conditions define the vector $\mathbf{y}$ to be

$$\mathbf{y}=\mathbf{k}\times\boldsymbol{\mu}/|\,\mathbf{k}\,||\,\boldsymbol{\mu}\,|,$$

and the third orthogonal vector $\mathbf{x}$ is

$$\mathbf{x}=(\mathbf{k}\times\boldsymbol{\mu})\times\mathbf{k}/k^2\,|\,\boldsymbol{\mu}\,|,$$

whereupon

$$\boldsymbol{\mu}\cdot\mathbf{R}/|\,\boldsymbol{\mu}\,||\,\mathbf{R}\,|=\boldsymbol{\mu}\cdot\mathbf{x}\cos\varphi\sin\vartheta+\boldsymbol{\mu}\cdot\mathbf{z}\cos\vartheta$$
$$=A\cos\varphi\sin\vartheta+B\cos\vartheta,$$

where φ and ϑ are the usual azimuthal and polar angles in a polar coordinate system with $\mathbf{k}$ along the polar axis. We consider, as an example, the integration of the term

$$\int_{R_0}^{R_f}\exp(i\mathbf{k}\cdot\mathbf{R})\left[\frac{1-3\cos^2(\boldsymbol{\mu}\cdot\mathbf{R})}{R^3}\right]d^3R,$$

which may be rewritten in the form

$$-\int_0^\pi\int_{R_0}^{R_f}\exp(i\,|\,\mathbf{k}\,|\,R\cos\vartheta)\frac{3(A^2\pi\sin^2\vartheta+2\pi B^2\cos^2\vartheta)-2\pi}{R}d(\cos\vartheta)dR. \quad \text{(A10)}$$

Now

$$\cos^2\vartheta=\tfrac{2}{3}[P_2(\cos\vartheta)+\tfrac{1}{2}P_0(\cos\vartheta)],$$
$$\sin^2\vartheta=\tfrac{2}{3}[P_0(\cos\vartheta)-P_2(\cos\vartheta)], \quad \text{(A11)}$$

$$j_n(z)=\frac{1}{2i^n}\int_0^\pi\exp(iz\cos\vartheta)P_n(\cos\vartheta)\sin\vartheta\,d\vartheta, \quad \text{(A12)}$$

whereupon

$$I=-4\pi\int_{R_0}^{R_f}[j_0(kR)(A^2+B^2-1)$$
$$+j_2(kR)(A^2-2B^2)]dR/R \quad \text{(A13)}$$

after using the fact that $j_0(x)=(\sin x)/x$. To complete

the integration we note that

$$\int\frac{j_{m+1}(z)}{1}dz=-\frac{j_m(z)}{z^m}\,;\qquad \frac{j_1(z)}{z}=j_2(z)+j_0(z).$$

Proceeding similarly with the other terms, we find, letting $x=kR$,

$$E=\frac{4\pi\mu^2}{V}\int_{x_0=kR_0}^{x_f=kR_f}x^2dx\left\{\frac{j_2(x)}{x^2}(\cos x+x\sin x)P_2 -\frac{\cos x}{3}\left[\frac{2j_0(x)+P_2J_2(x)}{x}\right]\right\}. \quad \text{(A14)}$$

After integration over x,

$$E=(4\pi\mu^2/V)\{-\tfrac{8}{3}P_2[j_0(2x)+j_2(2x)] +2P_2[\tfrac{1}{6}\sin^2x+(\sin 2x/2x)]+\tfrac{1}{3}\sin^2x\}_{x_0=kR_0}^{x_f=kR_f}. \quad \text{(A15)}$$

In our case, $x_0\approx 0$, and taking x_f to be very large,

$$E=(8\pi\mu^2/3V)P_2+(4\pi\mu^2/3V)(P_2+1)\sin^2x_f. \quad \text{(A16)}$$

The first term of Eq. (A16) is the interaction energy in the static dipole approximation (no retardation), and the second term is the correction due to retardation. Note that $\sin^2kR_f$ oscillates rapidly for small changes in R_f.

It is now necessary to examine more carefully the nature of our analysis. In effect, the system under investigation consists of a crystal and an incident light wave. This system is replaced by the equivalent system of a crystal containing an excitation wave. Now to compute the absorption function of the crystal, we use a Hamiltonian formalism. In that formalism, more particularly in Eq. (14) and similar matrix elements, it is valid to use the retarded dipole–dipole interaction provided that the dipoles are well localized and do not overlap. Within the tight binding formalism, such as is applicable to the molecular crystals considered here, this condition is fulfilled.

When a light wave is incident on a crystal, there are induced fields within the crystal which exactly cancel the incident wave and replace it with a different wave propagating with velocity c/n, where n is the refractive index of the crystal. Thus, in our calculation of the dipole field we have included not only that part of the field which leads to the direct interaction, but also that part of the field corresponding to radiation from the sphere. It is this radiation which leads to the oscillating term $\sin^2x_f$. For, the extent of reflection or transmission of the wave at the surface depends on the phase relations between the source and the surface. Thus, the term $\sin^2x_f$ corresponds to expected interference effects.

Now, for a macroscopic sample, the interaction energy cannot depend on the exact position of the surface, and it is therefore legitimate to replace $\sin^2x_f$ by its average value $\frac{1}{2}$. Under these conditions, the maximum contribution of the retardation term to the interaction energy is 20%. Moreover, the wave vector corresponding to propagation of the interaction should differ from the incident wave vector (which defines the modulation of the wavefunction) because of the presence of matter and, for any reasonable value of the effective refractive index, the corrections arising from retardation become smaller.

It is clear that complete resolution of the effects of retardation of the interaction requires further investigation, but we believe that we have shown that, to sufficient accuracy (i.e., accuracy much higher than corresponding to other approximations in the analysis), the retardation effects may be neglected. The dipole interaction energy then becomes, simply,

$$I_{dd}=(8\pi/V)\,|\,\mathfrak{y}^2\,|\,P_2(\cos\mathfrak{y}\cdot\mathbf{k})[j_0(kR_0)+j_2(kR_0)] =(8\pi/V)\,|\,\mathfrak{y}^2\,|\,P_2(\cos\mathfrak{y}\cdot\mathbf{k}) \quad \text{(A17)}$$

since kR_0 is very small.

APPENDIX III: DIPOLE SUMS FOR A CYLINDRICAL CRYSTAL

Let

$$I_{dd}=I_1+2I_2, \quad \text{(A18)}$$

$$I_1=\frac{1}{V_0}\int\int\int\rho d\rho dzd\varphi\,\exp(i\mathbf{k}\cdot\mathbf{R})\left[\frac{1-3\cos^2(\mathfrak{y}\cdot\mathbf{R})}{R^3}\right]. \quad \text{(A19)}$$

Take the $\mathbf{k}$ vector to be in the z direction (as it is in the experiments), and take the direction cosines of $\mathfrak{y}$ in the xyz coordinate system to be p_1, p_2, and p_3, respectively. Then

$$I_1=\frac{1}{V_0}\int_{\rho_0}^{L}\int_0^{a/2}\int_0^{2\pi}\rho d\rho dzd\varphi\,\exp(i\,|\,\mathbf{k}\,|\,z)\left[\frac{1-3(\rho p_1\cos\varphi+\rho p_2\sin\varphi+p_3z)^2/(\rho^2+z^2)}{(\rho^2+z^2)^{\frac{3}{2}}}\right]$$

$$=\frac{\pi}{V_0}\int_{\rho_0}^{L}\int_0^{a/2}\rho d\rho dz\,\exp(i\,|\,\mathbf{k}\,|\,z)\left[\frac{(2z^2-\rho^2)(1-3p_3^2)}{(\rho^2+z^2)^{\frac{5}{2}}}\right]$$

$$=-\frac{4\pi}{V_0}P_2(\cos\mathfrak{y}\cdot\mathbf{k})\int_0^{a/2}dz\,\exp(i\,|\,\mathbf{k}\,|\,z)\left[\frac{\rho^2}{(\rho^2+z^2)^{\frac{3}{2}}}\right]\Bigg|_{\rho=\rho_0}^{\rho=L}. \quad \text{(A20)}$$

As $L\to\infty$,

$$I_1=\frac{4\pi}{V_0}P_2(\cos\mathfrak{y}\cdot\mathbf{k})\int_0^{a/2}dz\frac{\rho_0^2\exp(i\mid\mathbf{k}\mid z)}{(\rho_0^2+z^2)^{\frac{3}{2}}}\,. \tag{A21}$$

Now if we consider the second part of the integral,

$$\begin{aligned}I_1&=\frac{1}{V_0}\int_0^L\int_{a/2}^M\int_0^{2\pi}\rho d\rho dz d\varphi\exp(i\mid\mathbf{k}\mid z)\left[\frac{1-3(\rho p_1\cos\theta+\rho p_2\sin\theta+p_3 z)^2/(\rho^2+z^2)}{(\rho^2+z^2)^{\frac{3}{2}}}\right]\\&=-\frac{4\pi}{V_0}P_2(\cos\mathfrak{y}\cdot\mathbf{k})\int_{a/2}^M dz\exp(i\mid\mathbf{k}\mid z)\left\{\frac{\rho^2}{(\rho^2+z^2)^{\frac{3}{2}}}\right\}\Bigg|_{\rho=0}^{\rho=L}\\&=-\frac{4\pi}{V_0}P_2(\cos\mathfrak{y}\cdot\mathbf{k})\int_{a/2}^M\frac{\exp(i\mid\mathbf{k}\mid z)\,L^2}{(L^2+z^2)^{\frac{3}{2}}}dz.\end{aligned} \tag{A22}$$

APPENDIX IV: GEOMETRY OF CRYSTALS

Anthracene crystallizes in the monoclinic space group $C_{2h}^5(P2_1/a)$ with two molecules per unit cell.[34] If we denote the long axis by L, the short axis by M, and the axis by M and the axis perpendicular to the plane by N, then the axes of one set of molecules have the following direction cosines in the systems **a**, **b**, **c**. The vector **c′** is along the axis perpendicular to the a, b plane. (**c** is inclined at an angle of 124°42′ to the **a** axis in anthracene.)

Anthracene first set $\quad L_1=\begin{pmatrix}-0.496\\-0.125\\+0.859\end{pmatrix},\quad M_1=\begin{pmatrix}-0.323\\-0.892\\-0.316\end{pmatrix},\quad N_1=\begin{pmatrix}-0.806\\+0.435\\0.402\end{pmatrix}.$

The axes of Molecule 2 are found from the above by reflection in a plane perpendicular to the **b** axis.

Anthracene second set $\quad L_2=\begin{pmatrix}-0.496\\+0.125\\+0.859\end{pmatrix},\quad M_2=\begin{pmatrix}-0.323\\+0.892\\-0.316\end{pmatrix},\quad N_2=\begin{pmatrix}+0.806\\+0.435\\+0.402\end{pmatrix}.$